Thermodynamics of feldspathoid solutions

Article *in* Contributions to Mineralogy and Petrology · February 1998

DOI: 10.1007/s004100050364

CITATIONS
15

READS
823

2 authors:

Richard Sack
OFM Research
83 PUBLICATIONS **6,590** CITATIONS
SEE PROFILE

Mark S. Ghiorso
OFM Research
187 PUBLICATIONS **11,515** CITATIONS
SEE PROFILE

Contrib Mineral Petrol (1998) 130: 256–274

Richard O. Sack · Mark S. Ghiorso

Thermodynamics of feldspathoid solutions

Received: 24 April 1997 / Accepted: 21 August 1997

Abstract We have developed models for the thermodynamic properties of nephelines, kalsilites, and leucites in the simple system $NaAlSiO_4 - KAlSiO_4 - Ca_{0.5}AlSiO_4 - SiO_2 - H_2O$ that are consistent with all known constraints on subsolidus equilibria and thermodynamic properties, and have integrated them into the existing MELTS software package. The model for nepheline is formulated for the simplifying assumptions that (1) a molecular mixing-type approximation describes changes in the configurational entropy associated with the coupled exchange substitutions $\square Si \Leftrightarrow NaAl$ and $\square Ca \Leftrightarrow Na_2$ and that (2) Na^+ and K^+ display long–range nonconvergent ordering between a large cation and the three small cation sites in the $Na_4Al_4Si_4O_{16}$ formula unit. Notable features of the model include the prediction that the mineral tetrakalsilite (''panunzite'', sensu stricto) results from anti-ordering of Na and K between the large cation and the three small cation sites in the nepheline structure at high temperatures, an average dT/dP slope of about 55°/kbar for the reaction

nepheline + kalsilite = tetrakalsilite (K-rich nepheline)

over the temperature and pressure ranges 800–1050 °C and 500–5000 bars, roughly symmetric (i.e. quadratic) solution behavior of the K–Na substitution along joins between fully ordered components in nepheline, and large positive Gibbs energies for the nepheline reciprocal reactions

$$\square Na_3Al_3Si_5O_{16} + \frac{3}{4}K_4Al_4Si_4O_{16} = \frac{3}{4}Na_4Al_4Si_4O_{16} + \square K_3Al_3Si_5O_{16}$$

and

$$\square CaNa_2Al_4Si_4O_{16} + \frac{1}{2}K_4Al_4Si_4O_{16} = \frac{1}{2}Na_4Al_4Si_4O_{16} + \square CaK_2Al_4Si_4O_{16},$$

and for the leucite reciprocal reaction

$$KAlSi_2O_6\square_{3/2} + H_2OAlSi_2O_6Na\square_{1/2} = NaAlSi_2O_6\square_{3/2} + H_2OAlSi_2O_6K\square_{1/2}.$$

R.O. Sack
Department of Earth and Atmospheric Sciences,
Purdue University, West Lafayette, IN 47907-1397

M.S. Ghiorso
Department of Geological Sciences,
Box 351310 University of Washington, Seattle, WA 98195-1310

Editorial responsibility: T.L. Grove

Introduction

Nepheline, leucite, and kalsilite are the three most common anhydrous framework silicates of the feldspathoid family, which includes the sodalite group (e.g., sodalite, cancrinite, hauyne, nosean), and is closely related to the zeolites derived from its members by hydrothermal metamorphism (e.g., analcime). Most commonly these feldspathoids are constituents of silica-poor igneous rocks, in which the most common associated minerals include olivine, augite, apatite, alkali feldspar, perovskite, and melilite, and some of which derive from among the deepest source regions contributing to volcanism on the surface of our planet. To date, there has been no serious effort to develop comprehensive thermodynamic models for the purpose of simulating the crystallization of these minerals from natural silicate liquids.

As part of an ongoing program to develop an internally consistent thermodynamic database for standard state and mixing properties of the common rock-forming minerals (e.g., Berman 1988; Sack and Ghiorso 1989, 1991a, b, 1994a–c; Ghiorso 1990a; Ghiorso and Sack 1991, 1995; Hirschmann 1991; Ghiorso et al. 1995), we have developed models for the thermodynamic properties of nepheline-, leucite-, and kalsilite-solid solutions

(ss) and integrated them into the MELTS software package of Ghiorso and Sack (1995). We demonstrate that the revised MELTS correctly predicts crystallization of nepheline-kalsilite and leucite solutions in numerous lava series including those from Ross Island, Antarctica (e.g., Goldich et al. 1975), San Venanzo, Umbria, Italy (e.g., Bannister et al. 1953), and the Bunyaruguru volcanic area, south-west Uganda (e.g., Combe and Holmes 1945). In a subsequent contribution we conduct a more thorough analysis of crystallization of alkalic lavas utilizing the revised MELTS (Ghiorso and Sack, work in preparation).

Systematics

Nepheline is the most chemically permissive and widespread of the anhydrous feldspathoids. It typically approximates the structural formula $(K^+, \square, Na^+)^{LS}(Na^+, K^+, Ca^{2+})_3^{SS}(Si^{4+}, Al^{3+})_8O_{16}$ (LS and SS are the large and small sites defined by six-membered rings of AlO_4 and SiO_4 tetrahedra) and exhibits $P6_3$ space group symmetry at room temperature with a unit cell containing 32 oxygens (e.g., Buerger et al. 1954). It is a member of a group of $P6_3$ minerals that includes tetrakalsilite (''panunzite'' sensu stricto, Merlino et al. 1985) and trikalsilite (Sahama and Smith 1957), hexagonal stuffed derivatives of tridymite in which successive layers of alumina and silica tetrahedra superimpose as in tridymite but which differ in the symmetry of the cavities accommodating alkali ions and **a** lattice parameters (e.g., Merlino 1984). In nepheline there is a 1:3 ratio of alkali sites with hexagonal and oval symmetries; these sites house K, vacancies, and Na ions, and, Na, K, and Ca ions, respectively. The **a** lattice parameters of nepheline are roughly twice those of kalsilite, a $P6_3$ hexagonal stuffed derivative of tridymite in which successive layers of alumina and silica tetrahedra are rotated 180° with respect each other so that they do not superimpose on each other as in tridymite (e.g., Perrota and Smith 1965; Palmer 1994). Trikalsilite and tetrakalsite have various combinations of alkali sites with hexagonal, ditrigonal, and oval symmetries (e.g., Bonaccorsi et al. 1988), and have **a** lattice parameters three and four times those of kalsilite.

The principal chemical substitution in natural nephelines is K for Na. At temperatures below around 800 °C the extent of K for Na exchange in nepheline is limited by saturation with kalsilite, and, depending on K/Na ratio, nepheline may coexist with alkali feldspar, leucite, and/or kalsilite in the simple system $NaAlSiO_4 - KAlSiO_4 - SiO_2$ (Figs. 1, 2; Hamilton and MacKenzie 1960, 1961). Above 800 °C phase relations are further complicated by the appearance of tetrakalsilite by a reaction between nepheline and kalsilite,

$$\text{nepheline} + \text{kalsilite} = \text{tetrakalsilite (K-rich nepheline)}, \quad (1)$$

at less than 2 kbar (e.g., Sahama 1957, 1962; Sahama and Smith 1957; Smith and Tuttle 1957; Tuttle and Smith 1958; Ferry and Blencoe 1978; Merlino et al. 1985; Bonaccorsi et al. 1988; Hovis et al. 1992; Hovis and Roux 1993; Carpenter and Cellai 1996; Fig. 2), and any resulting miscibility gap between tetrakalsilite and nepheline must disappear below about 1100° C (e.g., Tuttle and Smith 1958; Ferry and Blencoe 1978). In contrast, the substitution of K for Na apparently simplifies nepheline's structural systematics, as the changes in Na end-member from low to high nepheline (~810° C) and to carnegieite (1254° C) (e.g., Greig and Barth 1938) are not observed in nephelines with molar K/(K + Na) ratio greater than about 0.05 and 0.32, respectively (Tuttle and Smith 1958). Sodic nephelines also may exhibit a fairly substantial substitution towards SiO_2 (Fig. 1). This substitution is accomplished by the cou-

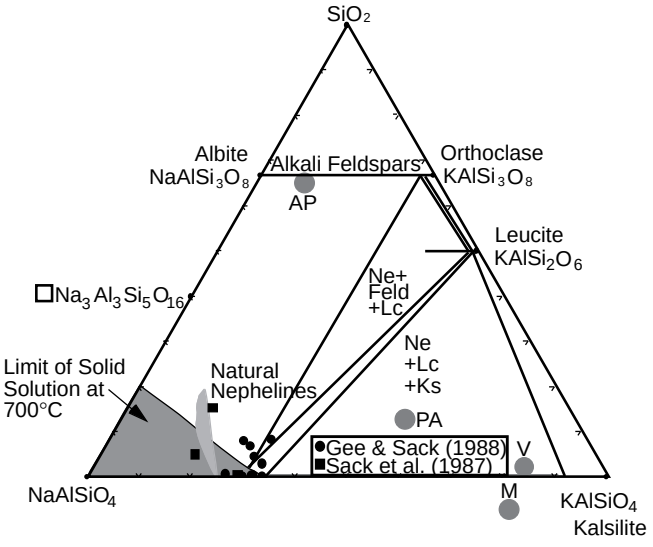

Fig. 1 Compositions of feldspathoids (nepheline, kalsilite, leucite) and alkali feldspars displayed in the composition plane defined by $NaAlSiO_4$, $KAlSiO_4$, and SiO_2. *Shaded area* adjacent to the $NaAlSiO_4$ vertex indicates the approximate limit of solid solution of nepheline towards SiO_2 at 700 °C (1 kbar) as defined by the experimental data of Hamilton and MacKenzie (1960) (cf. Fig. 3). *Cigar shaped area with rectangular pattern* extending between the compositions $K_{0.25}Na_{0.75}AlSiO_4$ and $\square Na_3Al_3Si_5O_{16}$ approximates the composition range of most natural nephelines as reported by Dollase and Thomas (1978). *Interior triangles* approximate compositional variables of three phase assemblages nepheline+ alkali feldspar + leucite (Ne + Feld + Lc) and nepheline + leucite+ kalsilite (Ne + Lc + Ks) at 700 °C (1 kbar). *Solid squares and circles* represent the compositions of nephelines produced in 1 atmosphere (QFM) melting and crystallization experiments on basic nephelinites by Sack et al. (1987a) and Gee and Sack (1988). They have been projected onto the $NaAlSiO_4 - KAlSiO_4 - SiO_2$ triangle through a $\square CaNa_2Al_4Si_4O_{16}$ component. *Shaded circles* indicate proportions of nepheline, kalsilite, and quartz normative components in an anorthoclase phonolite (*AP*, Goldich et al. 1975), potash ankaratrite (*PA*, Brown 1971), mafurite (*M*, Coomb and Holmes 1945, Table IV), and venanzite (*V*, Bannister et al. 1953, Table I) calculated for liquidus temperatures and oxygen fugacities defined by the QFM buffer (PM, M, &V) and one $\log_{10}$ unit below this buffer from the following algorithms (mol oxides):
$NaAlSiO_4 = 2Na_2O; KAlSiO_4 = 2K_2O;$
$SiO_2(\text{Quartz}) = SiO_2 + \frac{1}{2}(Al_2O_3 + Fe_2O_3 - FeO - MgO - 3CaO - 3Na_2O - 3K_2O - 10P_2O_5)$

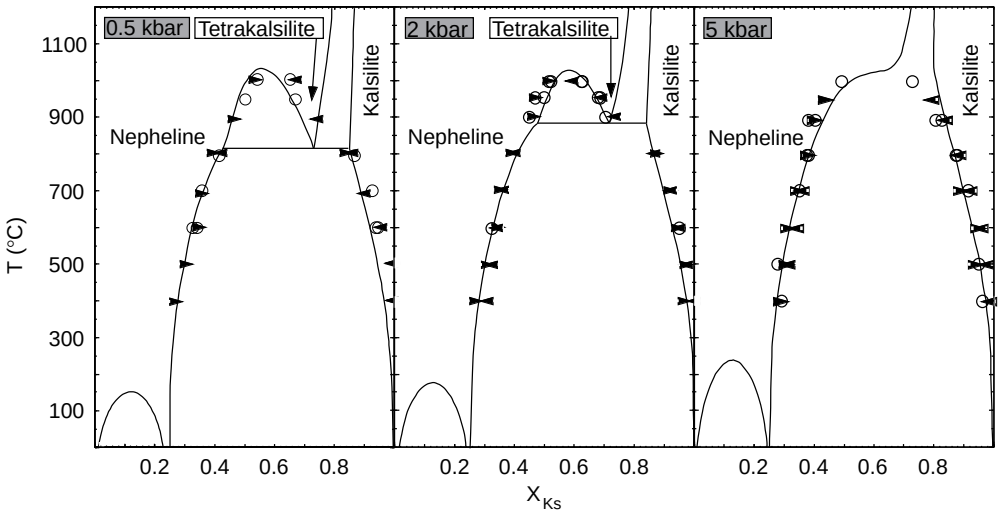

Fig. 2 Calculated miscibility gaps for $NaAlSiO_4$– $KAlSiO_4$ nephelines and kalsilites compared with experimental brackets of Ferry and Blencoe (1978). Symbols designate experimental products as follows: *open circles* synthesis, *pairs of inwards pointing arrows* homogenization, *pairs of outwards pointing arrows* unmixing experiments

pled exchange $NaAl \leftrightarrow \square Si$, or $\square Si(NaAl)_{-1}$, which transforms Na-nepheline end-member $Na_4Al_4Si_4O_{16}$ into a hypothetical end-member $\square Na_3Al_3Si_5O_{16}$ with fully vacant large alkali sites. The extent of this substitution depends strongly on temperature and Na/K ratio (Figs. 1, 3; Grieg and Barth 1938; Hamilton and MacKenzie 1960, 1961; Edgar 1964). Finally, magmatic nephelines may be enriched in Ca (e.g., Bowen 1912; Gee and Sack 1988). This substitution is accomplished by the coupled exchange $2\ Na \leftrightarrow \square Ca, \square Ca(Na_2)_{-1}$, which transforms Na-nepheline end-member $Na_4Al_4Si_4O_{16}$ into a hypothetical end-member $\square CaNa_2Al_4Si_4O_{16}$, also with fully vacant large alkali sites.

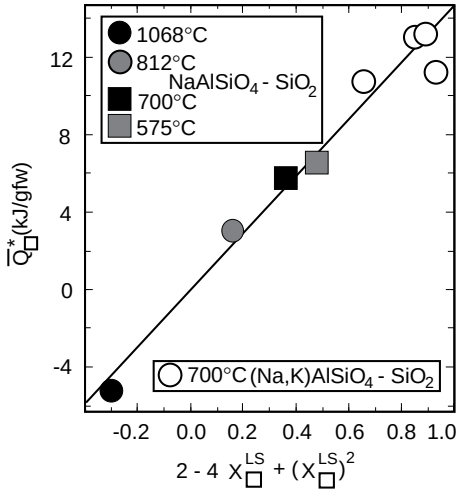

Fig. 3 Calibration of the condition of equilibrium of the reaction controlling the concentration of vacancies in nephelines coexisting with alkali feldspar (reaction 27) in the simple system $NaAlSiO_4 - KAlSiO_4 - SiO_2$ compared with experimental data of Grieg and Barth (1938), Edgar (1964), and Hamilton and MacKenzie (1960). This condition of equilibrium ($\overline{Q}^*_{\square}$) is expressed as a function of the mole fraction of vacancies in the large alkali site (LS) of nepheline ($X^{LS}_{\square} = X_3$ in this simple system) in zero intercept form with slope corresponding to the regular solution parameter $W_{\square Si-NaAl}$, and is given by Eq. A3 (Appendix)

Most natural nephelines have compositions near the plane defined by $KNa_3Al_4Si_4O_{16}$, $\square Na_3Al_3Si_5O_{16}$, and $\square CaNa_2Al_4Si_4O_{16}$ components (e.g., Barth 1963; Dollase and Thomas 1978) and the trace of this plane on the $NaAlSiO_4 - KAlSiO_4 - SiO_2$ ternary is at large acute angles with to respect curves which define the limits of solid solution of nephelines toward alkali feldspar at given temperatures (e.g., Fig. 1; Hamilton and MacKenzie 1960). It is particularly noteworthy that most of these nephelines most closely approximate the $KNa_3Al_4Si_4O_{16}$ composition, and that nephelines of this composition have strongly ordered cation distributions in which K strongly prefers to occupy the large hexagonal site (LS) and Na prefers to occupy the small oval sites (SS) (Buerger et al. 1954; Hahn and Buerger 1955). Stability of the ordered molecule $(K)^{LS}(Na)_3^{SS}Al_4Si_4O_{16}$ is further indicated by the fact the $KNa_3Al_4Si_4O_{16}$ composition defines a limit for the nepheline limb of the miscibility gap with decreasing temperature (Tuttle and Smith 1958; Ferry and Blencoe 1978; Fig. 2), and the point of inflection in volume-composition relations in nepheline-kalsilite solutions (e.g., Smith and Tuttle 1957, Donnay et al. 1959; Ferry and Blencoe 1978; Hovis et al. 1992; Fig. 4). Also noteworthy is the fact that synthetic tetrakalsilites have compositions clustering around $NaK_3Al_4Si_4O_{16}$, the composition of a nepheline fully anti-ordered in alkali distribution relative to the ordering scheme of $KNa_3Al_4Si_4O_{16}$ nephelines.

Kalsilites are simpler than nephelines in that they possess only one type of site (ditrigonal) on which alkalis substitute for each other, and they exhibit much more restricted ranges of the K/(K + Na) ratios and vacancy and Ca contents. The molar K/(K + Na) of kalsilites that can be readily synthesized, or are found in nature, is typically in the range 0.78 to 1.00 (e.g., Smith and Tuttle 1957; Deer et al. 1963; Hovis et al. 1992), although kalsilites with values of this ratio as low as 0.70 can apparently be obtained by rapid quench of high tem-

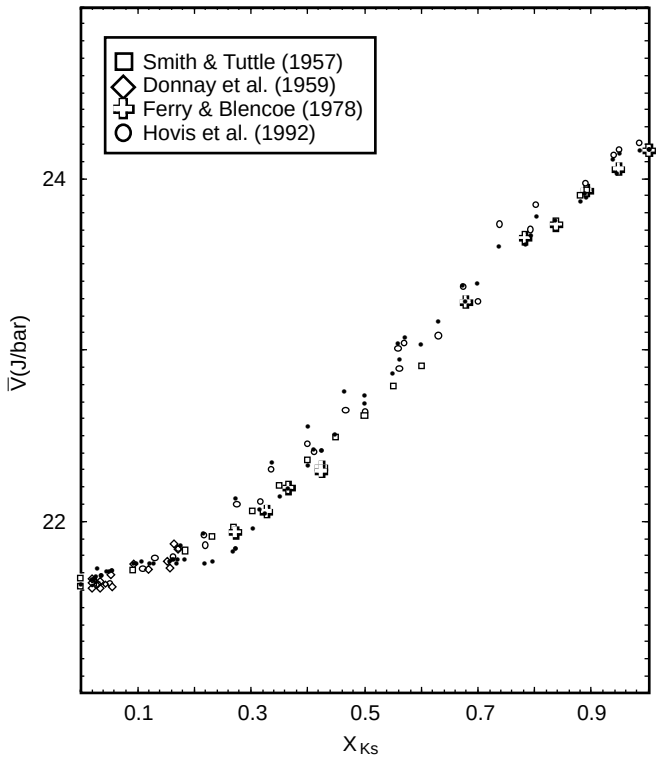

Fig. 4 Comparison of molar volumes of $Na_4Al_4Si_4O_{16}$ $-K_4Al_4Si_4O_{16}$ $-\square Na_3Al_3Si_5O_{16}$ $-\square CaNa_2Al_4Si_4O_{16}$ nephelines, tetrakalsilites, and kalsilites with calculated results. *Open squares*, *diamonds*, *crosses*, *and circles* indicate volumes determined by Smith and Tuttle (1957), Donnay et al. (1959), Ferry and Blencoe (1978) and Hovis et al. (1992) respectively. *Solid dots* are corresponding volumes calculated from expressions A4a,b (Appendix)

perature/pressure synthetics (Ferry and Blencoe 1978). Vacancy and Ca contents of the ditrigonal sites are typically less than several percent (e.g., Hamilton and MacKenzie 1960; Deer et al. 1963). End-member K-kalsilite undergoes at least one structural transition at high temperature, possibly exhibiting $P6_3mc$ space group symmetry by 950° C (e.g., Dollase and Freeborn 1977; Andou and Kawahara 1982; Abbott 1984; Kawahara et al. 1987; Carpenter and Cellai 1996), and this transition between $P6_3$ and $P6_3mc$ kalsilite structures may also involve a $P6_3$ nepheline-like phase with an **a** lattice parameter six times that of kalsilite (Carpenter and Cellai 1996). In addition to kalsilite there are also several other phases with compositions close to $KAlSiO_4$. These include kaliophilite, a hexagonal phase with an **a** lattice parameter roughly $3\sqrt{3}$ that of kalsilite, which is found in pyroclastic deposits (e.g., Bannister and Hey 1931; Smith and Tuttle 1957; Tuttle and Smith 1958), and orthorhombic (or possibly monoclinic?) O1-$KAlSiO_4$, a synthetic, possibly metastable, high temperature replacement for kalsilite (Smith and Tuttle 1957; Gregorkiewitz and Shäfer 1980; Abbott 1984; Cellai et al. 1992).

At room temperature leucite ($KAlSi_2O_6$) is tetragonal ($I4_1/a$, Mazzi et al. 1976), whereas above ~950 K, the structure is cubic (Ia3d, Peacor 1968). O atoms are found on symmetrically equivalent positions in the cubic structure ($Z = 16$) and are located among six sets of equivalent positions in the tetragonal cell. Si and Al are distributed over a framework of tetrahedral sites (a single equipoint in Ia3d) which are arranged into 4- and 6-membered rings, the latter of which are normal to the triad axes in the cubic structure. K^+ ions are 12-coordinated with O and occupy central locations within large channels formed by the six-membered rings. In addition, there are 24 smaller cavities in the unit cell (one and a half per formula unit) which are coordinated by four co-planar oxygens and two occupants of the larger (12-coordinated) sites. These cavities are vacant or may contain water molecules in leucite; two thirds of these positions are occupied by Na in isostructural analcime ($NaAlSi_2O_6 \cdot H_2O$; Taylor 1930), with H_2O taking the place of K on the large site.

The leucite structure can accommodate extensive substitution of Na for K (up to about 50 mol% $NaAlSi_2O_6$, Fudali 1963), but naturally occurring leucite solid solutions (leucite-ss) seldom contain more than 13 mol% $NaAlSi_2O_6$ (Deer et al. 1963). More sodic leucite-ss phenocrysts apparently breakdown to mixtures of nepheline and alkali-feldspar (pseudoleucite) on cooling (Fudali 1963). Ca substitution in leucite-ss is minor. In igneous rocks, leucite-ss (especially the more sodic varieties) are sometimes associated with analcime, some of which is interpreted as primary (Johannsen 1938; Luhr and Kyser 1989). Notable amounts of K (~ 25% $KAlSi_2O_6 \cdot H_2O$, Deer et al. 1963) is found in analcime associated with pseudoleucite. These observations bring to focus the likelihood and extent of solid solution between (Na,K) $AlSi_2O_6$ and the isostructural series (Na,K) $AlSi_2O_6 \cdot H_2O$ (e.g., Barrer 1982). Although the instability of $NaAlSi_2O_6 \cdot H_2O$ at higher temperatures argues against crystallization of this end-member under igneous conditions (Roux and Hamilton 1976), little is known regarding the stability relations of the K-end-member or any solid solutions of this series.

The polymorphic transition in leucite is complex, taking place over a variable temperature interval and involving the formation of an intermediate structure with probable symmetry $I4_1/acd$ (Wyart 1938, 1940; Lange et al. 1986). The transition(s) have been investigated by differential scanning calorimetry (Lange et al. 1986) and by other experimental techniques (Boysen 1990; Palmer 1990; Palmer et al. 1988, 1989, 1990; Palmer and Salje 1990) and multiple hypotheses for the mechanism of the phase transition have been advanced (Hatch et al. 1990; Palmer et al. 1990; Palmer and Salje 1990). Two phenomena appear to be operative: (1) Al–Si ordering over tetrahedral sites and (2) distortion and collapse of the Si–Al framework about the K^+ ions which are displaced from their symmetrical positions $(\frac{1}{8}\frac{1}{8}\frac{1}{8})$ in the cubic structure. Palmer et al. (1990) and Palmer and Salje (1990) argued that the Ia3d → $I4_1/acd$ transition is first order and is induced by a distortion of

the structure accompanied by Al–Si ordering ($I4_1/acd$ is a subgroup of Ia3d related by occupancy of the tetrahedral sites; Wyart 1938, 1940). They asserted that the $I4_1/acd \rightarrow I4_1/a$ transition may very well be second order, induced by displacement of K^+ ions from their central positions in the 6-member ring channels. Hatch et al. (1990) focused on the ubiquitous twinning found in tertragonal leucites and argued that the cubic structure is best viewed as a dynamical averaging of the six distinct {110}-type twin domains defining "pseudomerohedric" twins in $I4_1/acd$. In their model the twinning necessarily "freezes in" Al–Si ordering and displacement of K^+ ions. Further Al–Si ordering and displacement of K^+ induce the second tetragonal transition, which may very well be second order (Hatch et al. 1990).

Regardless of the controversy surrounding the precise mechanism of the structural transition in leucite, it is possible to infer the maximal configurational entropy (or "dynamical entropy") associated with the symmetry breaking transitions $Ia3d \rightarrow I4_1/acd$ and $I4_1/acd \rightarrow I4_1/a$. If the Ia3d structure is essentially a dynamical averaging of microscopic {110}-type twin domains of $I4_1/a$ symmetry (as suggested by Hatch et al. 1990 and supported by the neutron scattering studies of Boysen 1990), then the entropy of the transition is related to the multiplicity factor for {110}in Ia3d ratioed to that in $I4_1/a$. This is R ln(12), or about 20.66 J/mol-K. This configurational entropy need not be developed entirely at the transition, but could be spread over a considerable temperature range, as is the case with the polymorphs of silica (e.g., Ghiorso et al. 1979). For example, Lange et al. (1986) attributed an entropy of only $3-4$ J/K-mol for the cumulative effect over a range of $\sim$100 K of the $Ia3d \rightarrow I4_1/a$ transition, less than a fifth of the inferred theoretical entropy. If additional configurational entropy develops through a mechanism related to $Al-Si$ ordering, then accurate experimental assessment of the temperature dependence of the thermodynamic consequences of the leucite structural phase transition, may in fact be extremely difficult, as the kinetics of this tetrahedral ordering process may be very sluggish. We will return to this issue below in the section on calibration.

Thermodynamics

The systematics summarized above may be readily accounted for with internally consistent thermochemical models for the feldspathoids nepheline, kalsilite, and leucite providing we make explicit provision for the stability of the ordered molecule $(K)^{LS}(Na)_3^{SS}Al_4Si_4O_{16}$ in the formulation for the thermodynamic properties of nephelines and for the incompatibility between H_2O and K in leucite. In this section we first outline our formulation of such a model for nepheline and simpler models for kalsilites and leucites. We then discuss the calibration of the parameters of these models based on experimental and natural constraints.

Formulation

Nepheline-tetrakalsilite

We consider a composition space defined by the nepheline end-member, $Na_4Al_4Si_4O_{16}$, and the exchange components $K(Na)_{-1}$, $\square Si(NaAl)_{-1}$, and $\square Ca(Na)_{-2}$ adequate to account for first order compositional variations in nepheline-tetrakalsilite solutions. We assume that nepheline and tetrakalsilite exhibit continuous behavior in thermodynamic properties at temperatures appropriate to magmatic processes, and restrict our attention to nephelines with sufficient $\square$ and K that they crystallize in the low nepheline structural state. For nepheline we also assume that (1) vacancies and Ca^{2+} are respectively restricted to the large cation and small cation sites, respectively (e.g., Hovis et al. 1992; Hovis and Roux 1993), (2) Al^{3+} and Si^{4+} have a fully short-range ordered distribution in tetrahedral sites (Stebbins et al. 1986; Hovis et al. 1992), and (3) K^+ and Na^+ display long-range, non-convergent ordering between the large cation and small cation sites. For these assumptions, we define the following set of linearly independent composition variables:

$$X_2 \equiv \frac{1}{4}X^{LS}_{K^+} + \frac{3}{4}X^{SS}_{K^+} \tag{2a}$$

$$X_3 \equiv X^{LS}_{\square} - 3X^{SS}_{Ca^{2+}} \tag{2b}$$

$$X_4 \equiv 3X^{SS}_{Ca^{2+}} \tag{2c}$$

and the following ordering variable:

$$s_1 \equiv (X^{LS}_{K^+} - X^{SS}_{K^+}), \tag{3}$$

Given the site population constraints:

$$1 = X^{LS}_{Na^+} + X^{LS}_{K^+} + X^{LS}_{\square} \tag{4a}$$

$$1 = X^{SS}_{Na^+} + X^{SS}_{K^+} + X^{SS}_{Ca^{2+}}, \tag{4b}$$

the following expressions that relate the mole fractions of cations on large (LS) and small (SS) alkali sites composition and ordering variables may be readily derived:

$$X^{LS}_{K^+} = X_2 + \frac{3}{4}\,s, \qquad X^{SS}_{K^+} = X_2 - \frac{1}{4}\,s$$

$$X^{LS}_{\square} = X_3 + X_4 \qquad X^{SS}_{Ca^{2+}} = \frac{1}{3}X_4$$

$$X^{LS}_{Na^+} = 1 - X_2 - X_3 - X_4 - \frac{3}{4}\,s \qquad X^{SS}_{Na^+} = 1 - X_2 - \frac{1}{3}X_4 + \frac{1}{4}\,s. \tag{5}$$

For the assumption that the ideal molar configurational entropies $(\overline{S}^{IC})$ for coupled substitutions may be satisfactorily approximated with molecular mixing approximations of the type

$$\overline{S}^{IC} = -R\sum_i X_i \ \ln\ X_i, \tag{6}$$

(R is the universal gas constant), we may readily derive an expression for $(\overline{S}^{IC})$ for nephelines expressed in terms of the ordering and composition variables X_2, X_3, X_4, and s (Table 2).

Table 1 Linearly independent thermodynamic parameters for nepheline solutions

Parameter Type	Label	Definition
End-member components	$\overline{G}_1^*$	$\overline{G}^0_{Na_4Al_4Si_4O_{16}}$
	$\overline{G}_2^*$	$\overline{G}^0_{K_4Al_4Si_4O_{16}}$
	$\overline{G}_3^*$	$\overline{G}^0_{\square Na_3Al_3Si_5O_{16}}$
	$\overline{G}_4^*$	$\overline{G}^*_{\square CaNa_2Al_4Si_4O_{16}}$
Ordering energy	$\Delta\overline{G}^0_{EX}$	$\overline{G}^0_{KNa_3Al_4Si_4O_{16}} + \frac{1}{2}\overline{G}^0_{K_4Al_4Si_4O_{16}} - \overline{G}^0_{NaK_3Al_4Si_4O_{16}} - \frac{1}{2}\overline{G}^0_{Na_4Al_4Si_4O_{16}}$
Reciprocal energies	$\Delta\overline{G}^0_{23}$	$\overline{G}^0_{\square K_3Al_3Si_5O_{16}} + \frac{3}{4}\overline{G}^0_{Na_4Al_4Si_4O_{16}} - \overline{G}^0_{\square Na_3Al_3Si_5O_{16}} - \frac{3}{4}\overline{G}^0_{K_4Al_4Si_4O_{16}}$
	$\Delta\overline{G}^0_{24}$	$\overline{G}^0_{\square CaK_2Al_4Si_4O_{16}} + \frac{1}{2}\overline{G}^0_{Na_4Al_4Si_4O_{16}} - \overline{G}^0_{\square CaNa_2Al_4Si_4O_{16}} - \frac{1}{2}\overline{G}^0_{K_4Al_4Si_4O_{16}}$
Reciprocal ordering energy	$\Delta\overline{G}^0_X$	$\overline{G}^0_{KNa_3Al_4Si_4O_{16}} + \overline{G}^0_{NaK_3Al_4Si_4O_{16}} - \overline{G}^0_{K_4Al_4Si_4O_{16}} - \overline{G}^0_{Na_4Al_4Si_4O_{16}}$
Symmetric regular solution parameters		Relevant join(s)
	$W_{\square Si—NaAl}$	$\square Na_3Al_3Si_5O_{16} - Na_4Al_4Si_4O_{16}$ $\square K_3Al_3Si_5O_{16} - NaK_3Al_4Si_4O_{16}$
	$W_{\square Si—KAl}$	$\square K_3Al_3Si_5O_{16} - K_4Al_4Si_4O_{16}$ $\square Na_3Al_3Si_5O_{16} - KNa_3Al_4Si_4O_{16}$
	$W^{LS}_{Na—K}$	$KNa_3Al_4Si_4O_{16} - Na_4Al_4Si_4O_{16}$ $K_4Al_4Si_4O_{16} - NaK_3Al_4Si_4O_{16}$
	$W^{SS}_{Na—K}$	$NaK_3Al_4Si_4O_{16} - Na_4Al_4Si_4O_{16}$ $K_4Al_4Si_4O_{16} - KNa_3Al_4Si_4O_{16}$
	$W_{\square Ca—Na_2}$	$\square CaNa_2Al_4Si_4O_{16} - Na_4Al_4Si_4O_{16}$
	$W_{\square Ca—K_2}$	$\square CaK_2Al_4Si_4O_{16} - K_4Al_4Si_4O_{16}$
	$W_{CaAl—NaSi}$	$\square CaNa_2Al_4Si_4O_{16} - \square Na_3Al_3Si_5O_{16}$

In our formulation, the molar Gibbs energy ($\overline{G}$) is given by the equation

$$\overline{G} = \overline{G}^* - T\overline{S}^{IC}, \tag{7}$$

where $\overline{G}^*$ is the *vibrational* Gibbs energy and this expression for $\overline{S}^{IC}$. We assume that $\overline{G}^*$ may be described using a Taylor expansion of second degree in the composition (X_i's) and ordering (s) variables defined by Eqs. 2 and 3

$$\overline{G}^* = g_0 + \sum_i [g_i X_i + g_{ii} X_i^2 + \sum_{j<i} g_{ij} X_i X_j] + \sum_i [g_{is} X_i s] + g_s s + g_{ss} s^2 \tag{8}$$

We next adopt a linearly independent set of thermodynamic parameters (Table 1), analogous to those employed by Sack and Ghiorso (1991a, 1994a), comprising (1) the 'vibrational' Gibbs energies of the linearly independent set of end-members $Na_4Al_4Si_4O_{16}$, $K_4Al_4Si_4O_{16}$, $\square Na_3Al_3Si_5O_{16}$, and $\square CaNa_2Al_4Si_4O_{16}$, all referred to the $P6_3$ structure; (2) differences between the Gibbs energies of ordered and anti-ordered component pairs $(K)^{LS}(Na)_3^{SS}$ $Al_4Si_4O_{16}$ and $(Na)^{LS}(K)_3^{SS}Al_4Si_4O_{16}$ and those of K- and Na-end-members given by the reciprocal and reciprocal-ordering reactions

$$(Na)^{LS}(K)_3^{SS}Al_4Si_4O_{16} + \frac{1}{2}Na_4Al_4Si_4O_{16} = \frac{1}{2}K_4Al_4Si_4O_{16} + (K)^{LS}(Na)_3^{SS}Al_4Si_4O_{16} \tag{9}$$

$$Na_4Al_4Si_4O_{16} + K_4Al_4Si_4O_{16} = (K)^{LS}(Na)_3^{SS}Al_4Si_4O_{16} + (Na)^{LS}(K)_3^{SS}Al_4Si_4O_{16}; \tag{10}$$

(3) the Gibbs energies of reciprocal reactions expressing the compositions of dependent components $\square K_3Al_3Si_5O_{16}$ and $\square CaK_2Al_4Si_4O_{16}$ in terms of the linearly independent set of end-members

$$\square Na_3Al_3Si_5O_{16} + \frac{3}{4}K_4Al_4Si_4O_{16} = \frac{3}{4}Na_4Al_4Si_4O_{16} + \square K_3Al_3Si_5O_{16} \tag{11}$$

$$\square CaNa_2Al_4Si_4O_{16} + \frac{1}{2}K_4Al_4Si_4O_{16} = \frac{1}{2}Na_4Al_4Si_4O_{16} + \square CaK_2Al_4Si_4O_{16}; \tag{12}$$

and (4) symmetric regular-solution-type (Margules) parameters (W_{i-j}) describing deviations from linearity in *vibrational* Gibbs energy of mixing along joins between vertices of composition-ordering space. These parameters are identified with the Taylor coefficients in the usual manner, and they result in the expression for $\overline{G}^*$ appearing in the top eight lines of Table 2. We may also extend the expression for $\overline{G}^*$ (Eq. 8) to third degree in composition and ordering variables to make explicit provision for the asymmetry in mixing of K- and Na-end-member components that is typically invoked in treating the thermodynamic properties of alkali feldspars (e.g., Thompson and Waldbaum 1969; Luth and Fenn 1973; Helgeson et al. 1978; Thompson and Hovis 1979; Haselton et al. 1983; Ghiorso 1984; Fuhrman and Lindsley 1988; Elkins and Grove 1990; Hovis et al. 1991). We have found that this activity is unneccesary in a first-order description, and therefore will not pursue this matter further[1].

[1]The interested reader may obtain the results of the third-degree expansion from the authors.

Table 2 Definition of $\overline{G}$ in terms of the preferred thermodynamic parameters

$$\begin{aligned}
\overline{G}^{*} &= \overline{G}^{0}_{Na_4Al_4Si_4O_{16}}(1-X_2-X_3-X_4)+\overline{G}^{0}_{K_4Al_4Si_4O_{16}}(X_2)+\overline{G}^{0}_{\square Na_3Al_3Si_5O_{16}}(X_3)+\overline{G}^{*}_{\square CaNa_2Al_4Si_4O_{16}}(X_4)\\
&+\frac{1}{4}\left[2\,\Delta\overline{G}^{0}_{EX}+\Delta\overline{G}^{0}_{X}+3\,W^{LS}_{Na-K}-W^{SS}_{Na-K}\right](s)+\left[\Delta\overline{G}^{0}_{X}+W^{LS}_{Na-K}+W^{SS}_{Na-K}\right](X_2)(1-X_2)\\
&+\frac{1}{16}\left[3\,\Delta\overline{G}^{0}_{X}-9\,W^{LS}_{Na-K}-W^{SS}_{Na-K}\right](s^2)-\frac{1}{2}\left[\Delta\overline{G}^{0}_{X}+3\,W^{LS}_{Na-K}-W^{SS}_{Na-K}\right](X_2)(s)+W_{\square Si-NaAl}(X_3)(1-X_3)\\
&+\frac{1}{2}\left[2\,\Delta\overline{G}^{0}_{23}+\Delta\overline{G}^{0}_{EX}-\Delta\overline{G}^{0}_{X}-2\,W^{LS}_{Na-K}-2\,W_{\square Si-NaAl}+2\,W_{\square Si-KAl}\right](X_2)(X_3)\\
&+\frac{1}{8}\left[\Delta\overline{G}^{0}_{X}-\Delta\overline{G}^{0}_{EX}-2\,\Delta\overline{G}^{0}_{23}-6\,W^{LS}_{Na-K}-6\,W_{\square Si-NaAl}+6\,W_{\square Si-KAl}\right](X_3)(s)+W_{\square Ca-Na_2}(X_4)(1-X_4)\\
&+\frac{1}{3}(3\,\Delta\overline{G}^{0}_{24}+\Delta\overline{G}^{0}_{EX}-2\,\Delta\overline{G}^{0}_{X}-3\,W^{LS}_{Na-K}-W^{SS}_{Na-K}+3\,W_{\square Ca-K_2}-3\,W_{\square Ca-Na_2})(X_2)(X_4)\\
&+(W_{CaAl-NaSi}-W_{\square Ca-Na_2}-W_{\square Si-NaAl})(X_3)(X_4)\\
&+\frac{1}{12}(9\,W_{\square Ca-K_2}-9\,W_{\square Ca-Na_2}-9\,W^{LS}_{Na-K}+W^{SS}_{Na-K}-3\,\Delta\overline{G}^{0}_{EX}-9\,\Delta\overline{G}^{0}_{24})(X_4)(s)\\
\overline{S}^{IC} &= -R\left\{\left[X_2+\frac{3}{4}s\right]\ln\left\{X_2+\frac{3}{4}s\right\}+(X_3-X_4)\ln\{X_3-X_4\}+\left(1-X_2-X_3-X_4-\frac{3}{4}s\right)\ln\left\{1-X_2-X_3-X_4-\frac{3}{4}s\right\}\right.\\
&\left.-(1-X_4)\ln\{1-X_4\}+3\left(X_2-\frac{1}{4}s\right)\ln\left\{X_2-\frac{1}{4}s\right\}+X_4\ln\left\{\frac{1}{3}X_4\right\}+3\left(1-X_2-\frac{1}{3}X_4+\frac{1}{4}s\right)\ln\left\{1-X_2-\frac{1}{3}X_4+\frac{1}{4}s\right\}\right\}\\
\overline{G} &= \overline{G}^{*}-T\overline{S}^{IC}
\end{aligned}$$

Given the expression for $\overline{G}$ in Table 2, expressions for the chemical potentials of nepheline end-member components are readily derived by application of an extended form of the so-called Darken equation (Darken and Gurry 1953; Sack 1982; Sack et al. 1987b; Ghiorso 1990b)

$$\mu_j=\overline{G}+\sum_i n_{ij}(1-X_i)(\partial\overline{G}/\partial X_i)_{X_k/X_{l,s}}+\sum_i(q_{ij}-s)(\partial\overline{G}/\partial s)_{X_i,X_k} \tag{13}$$

where n_{ij} and q_{ij} refer to the values of X_i and s, respectively, in one mole of nepheline component j. Equilibrium values of the order variable are evaluated by setting the derivative $(\partial\overline{G}/\partial s)$ equal to zero and solving the resulting non-linear equation for s:

$$\begin{aligned}
RT\ln\left[\left\{\frac{X^{LS}_{Na^+}}{X^{LS}_{K^+}}\right\}\left\{\frac{X^{SS}_{K^+}}{X^{SS}_{Na^+}}\right\}\right] &= \frac{2}{3}\,\Delta\overline{G}^{0}_{EX}\\
&+\frac{1}{6}\left[3\,\Delta\overline{G}^{0}_{X}-9\,W^{LS}_{Na-K}-W^{SS}_{Na-K}\right](s)\\
&+\frac{1}{3}\left[\Delta\overline{G}^{0}_{X}+3\,W^{LS}_{Na-K}-W^{SS}_{Na-K}\right](1-2X_2)\\
&+\frac{1}{6}\left[\Delta\overline{G}^{0}_{X}-\Delta\overline{G}^{0}_{EX}-2\,\Delta\overline{G}^{0}_{23}-6\,W^{LS}_{Na-K}\right.\\
&\left.-6\,W_{\square Si-NaAl}+6\,W_{\square Si-KAl}\right](X_3)\\
&+\frac{1}{9}\left[9\,W_{\square Ca-K_2}-9\,W_{\square Ca-Na_2}\right.\\
&\left.-9\,W^{LS}_{Na-K}+W^{SS}_{Na-K}-3\,\Delta\overline{G}^{0}_{EX}-9\,\Delta\overline{G}^{0}_{24}\right](X_4).
\end{aligned}\tag{14}$$

Kalsilite

For kalsilite, we define the following set of linearly independent composition variables:

$$X_2\equiv X^{DS}_{K^+} \tag{15a}$$

$$X_3\equiv 4\,X^{DS}_{\square}-4\,X^{DS}_{Ca^{2+}} \tag{15b}$$

$$X_4\equiv 4\,X^{DS}_{Ca^{2+}}. \tag{15c}$$

Given the site population constraint:

$$1=X^{DS}_{Na^+}+X^{DS}_{K^+}+X^{DS}_{\square}+X^{DS}_{Ca^{2+}}, \tag{16}$$

the following expressions that relate the mole fractions of cations and vacancies on the ditrigonal (DS) site to composition variables may be readily derived:

$$\begin{aligned}
&X^{DS}_{K^+}=X_2,\quad X^{DS}_{\square}=\frac{1}{4}(X_3+X_4)\\
&X^{DS}_{Ca^{2+}}=\frac{1}{4}X_4\quad X^{DS}_{Na^+}=1-X_2-\frac{1}{4}X_3-\frac{1}{2}X_4.
\end{aligned}\tag{17}$$

For assumptions analogous to those employed for nepheline, we may readily obtain the following approximation for the molar configurational entropy ($\overline{S}^{IC}$) of the kalsilite

$$\begin{aligned}
\overline{S}^{IC} &= -R\left\{4\,X_2\ln\{X_2\}+(X_3)\ln\frac{1}{4}\{X_3\}+X_4\ln\frac{1}{4}\{X_4\}\right.\\
&\left.+4(1-X_2-\frac{1}{4}X_3+\frac{1}{2}X_4)\ln\{1-X_2-\frac{1}{4}X_3+\frac{1}{2}X_4\}\right\}
\end{aligned}\tag{18}$$

expressed in terms of the composition variables defined by Eqs. 17. Finally, we will assume that kalsilite behaves as a strictly regular solution for which

$$\begin{aligned}
\overline{G}^{*} &= \overline{G}^{*}_{Na_4Al_4Si_4O_{16}}(1-X_2-X_3-X_4)+\overline{G}^{*}_{K_4Al_4Si_4O_{16}}(X_2)\\
&+\overline{G}^{*}_{\square Na_3Al_3Si_5O_{16}}(X_3)\\
&+\overline{G}^{*}_{\square CaNa_2Al_4Si_4O_{16}}(X_4)+W^{KALS}_{Na-K}(1-X_2)(X_2)\\
&+W^{KALS}_{\square Si-NaAl}(1-X_3)(X_3)\\
&+W^{KALS}_{\square Ca-Na_2}(1-X_4)(X_4)+(W^{KALS}_{\square Na_3Si-K_4Al}-W^{KALS}_{\square Si-NaAl}\\
&-W^{KALS}_{Na-K})(X_2)(X_3)\\
&+(W^{KALS}_{\square CaNa_2-K_4}-W^{KALS}_{\square Ca-Na_2}-W^{KALS}_{Na-K})(X_2)(X_4)\\
&+(W^{KALS}_{CaAl-NaSi}-W^{KALS}_{\square Ca-Na_2}-W^{KALS}_{\square Si-NaAl})(X_3)(X_4)
\end{aligned}\tag{19}$$

and we combine Eqs. 18 and 19 according to Eq. (7) to obtain an expression for $\overline{G}$.

Leucite

We formulate a thermodynamic model for the cubic-structural state of leucite-ss in the composition space $(Na.K)^{LS}AlSi_2O_6(\square)^{SS}_{3/2}$–$(H_2O)^{LS}AlSi_2O_6(Na.K)^{SS}(\square)^{SS}_{1/2}$, where the superscript "LS" denotes the large 12-coordinated site and "SS" refers to the smaller, irregular, six-coordinated site (see above). $\square$ denotes a site vacancy. Recognizing that the thermodynamics of this system is best formulated as a reciprocal solution, we adopt as independent compositional variables r_K and r_{H_2O}, which denote respectively the number of moles of K and H_2O in the formula unit. Definitions for site mole fractions follow immediately from this designation:

$$\begin{aligned} X^{LS}_{K^+} &= r_K(1-r_{H_2O}) \\ X^{LS}_{Na^+} &= (1-r_K)(1-r_{H_2O}) \\ X^{LS}_{H_2O} &= r_{H_2O} \\ X^{SS}_{K^+} &= \frac{2}{3} r_K r_{H_2O} \\ X^{SS}_{Na^+} &= \frac{2}{3}(1-r_K) r_{H_2O} \\ X^{SS}_{\square} &= 1 - \frac{2}{3} r_{H_2O} \end{aligned} \tag{20}$$

The configurational entropy of these solutions may be written:

$$\begin{aligned} \overline{S}^{IC} = &-R\left(X^{LS}_{K^+}\ln X^{LS}_{K^+} + X^{LS}_{Na^+}\ln X^{LS}_{Na^+} + X^{LS}_{H_2O}\ln X^{LS}_{H_2O}\right) \\ &-\frac{3}{2}R\left(X^{SS}_{K^+}\ln X^{SS}_{K^+} + X^{SS}_{Na^+}\ln X^{SS}_{Na^+} + X^{SS}_{\square}\ln X^{SS}_{\square}\right) \end{aligned} \tag{21}$$

which simplifies upon substitution of the site definitions to:

$$\begin{aligned} \overline{S}^{IC} = -R\Big\{ &(r_K \ln r_K + (1-r_K)\ln(1-r_K) + 2\, r_{H_2O}\ln r_{H_2O} \\ &+ (1-r_{H_2O})\ln(1-r_{H_2O}) \\ &+ \left(\frac{3}{2}-r_{H_2O}\right)\ln\left(\frac{3}{2}-r_{H_2O}\right) + \frac{3}{2}\ln\frac{2}{3}\Big\} \end{aligned} \tag{22}$$

The molar Gibbs free energy of solution, $\overline{G}$, is expressed in the usual way (Eq. 7), where $\overline{G}^*$ is expanded as a second order Taylor series in the independent compositional variables. We adopt as model parameters the standard state Gibbs free energies of $KAlSi_2O_6\,\square_{3/2}(\overline{G}^0_{LC})$, $NaAlSi_2O_6\square_{3/2}\ (\overline{G}^0_{Na-LC})$, $H_2OAlSi_2O_6Na\,\square_{1/2}(\overline{G}^0_{AN})$, and the reciprocal exchange reaction:

$$\begin{aligned} KAlSi_2O_6\square_{3/2} + H_2OAlSi_2O_6Na\square_{1/2} &= NaAlSi_2O_6\square_{3/2} \\ &+ H_2OAlSi_2O_6K\square_{1/2}\left(\Delta\overline{G}^0_r\right), \end{aligned} \tag{23}$$

as well as regular solution-type interaction terms for the Na–K and (Na, K)–H_2O joins: W^{LC}_{Na-K} and $W^{LC}_{Na,K-H_2O}$. Identifying Taylor coefficients of $\overline{G}^*$ with these parameters results in our model expression for the molar Gibbs free energy of leucite-ss:

$$\begin{aligned} \overline{G} = &-T\overline{S}^{IC} + \overline{G}^0_{Na-LC}(1-r_K-r_{H_2O}) + \overline{G}^0_{LC}(r_K) + \overline{G}^0_{AN}(r_{H_2O}) \\ &+ \Delta\overline{G}^0_r(r_K)(r_{H_2O}) \quad + W^{LC}_{Na-K}(r_K)(1-r_K) \\ &+ W^{LC}_{Na,K-H_2O}(r_{H_2O})(1-r_{H_2O}) \end{aligned} \tag{24}$$

Calibration

Calibration of thermodynamic models for the anhydrous feldspathoids logically proceeds with nephelines and kalsilites approximating the $NaAlSiO_4$–$KAlSiO_4$ subsystem. Most of the mixing parameters of $NaAlSiO_4$–$KAlSiO_4$ nephelines and kalsilites are tightly constrained by brackets on miscibility gaps (Ferry and Blencoe 1978; Fig. 2), and measurements of enthalpies of solution (Hovis and Roux 1993; Fig. 5) and volumes (Smith and Tuttle 1957; Ferry and Blencoe 1978; Hovis et al. 1992; Fig. 4). We first calibrate these parameters and the differences in Gibbs energies between Na- and K-end-members with the nepheline and kalsilite structures ($\Delta\overline{G}^0_1$ and $\Delta\overline{G}^0_2$, Table 3) under the assumptions of identical heat capacities of Na-kalsilites and nephelines ($\Delta Cp_1 = 0$) and K-kalsilites and nephelines ($\Delta Cp_2 = 0$). We next obtain parameters for SiO_2-substituted nephelines and kalsilites and for the enthalpy of formation of

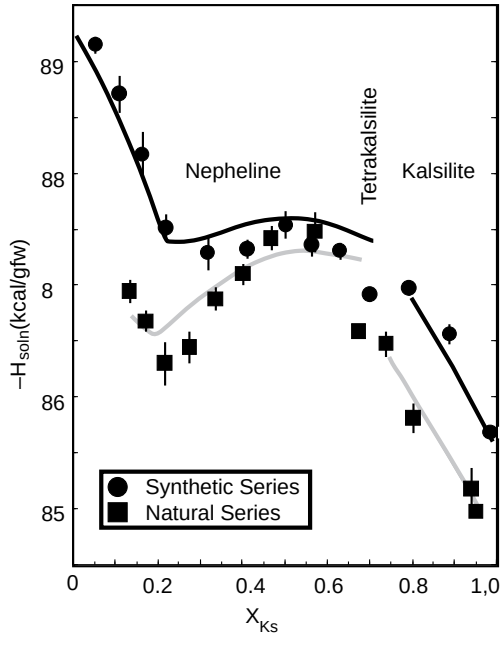

Fig. 5 Comparison of molar enthalpy of solution data of Hovis and Roux (1993) for $NaAlSiO_4 - KAlSiO_4 - \square_{0.25}Na_{0.75}Al_{0.75}Si_{1.25}O_4 - \square_{0.25}Ca_{0.25}Na_{0.5}AlSiO_4$ solutions with calculated results. *Circles and squares* represent data for nephelines ($0 < X_2 < 0.66$), tetrakalsilites ($0.70 < X_2 < 0.74$), and kalsilites ($0.75 < X_2 < .985$) of the synthetic ($X_3 \sim 0.07$) and natural ($X_3 \sim 0.21$) series, respectively. *Solid and dashed curves* represent curves calculated for the nephelines and kalsilites of these series using the parameter values given in Table 3, expressions A5a and A5b, and the end-member enthalpies of solution the end-members given in the Appendix

Table 3 Preferred values of solution parameters for $Na_4Al_4Si_4O_{16}$ – $K_4Al_4Si_4O_{16}$ – $\square Na_3Al_3Si_5O_{16}$ – $\square CaNa_2Al_4Si_4O_{16}$ nephelines and kalsilites and for $(K, Na)AlSi_2O_6(H_2O)$ leucites

Parameter	Value	Parameter	Value
$\Delta\overline{H}^0_{EX}$	−31.744 kJ/mol	$W^{SS}_{V\ Na-K}$	0.54392 J/bar
$\Delta\overline{S}^0_{EX}$	−20.920 J/K-mol	$W_{\square Si-NaAl}$	14.644 kJ/mol
$\Delta\overline{V}^0_{EX}$	−1.04600 J/bar	$W_{\square Si-KAl}$	8.368 kJ/mol
$\Delta\overline{H}^0_{X}$	−13.893 kJ/mol	$W_{\square Ca-Na_2}$	0.000 kJ/mol
$\Delta\overline{S}^0_{X}$	12.552 J/K-mol	$W_{\square Ca-K_2}$	0.000 kJ/mol
$\Delta\overline{V}^0_{X}$	0.00000 J/bar	$W_{CaAl-NaSi}$	0.000 kJ/mol
$\Delta\overline{H}^0_{23}$	73.520 kJ/mol	W^{KALS}_{Na-K}	29.288 kJ/mol
$\Delta\overline{S}^0_{23}$	0.000 J/K-mol	$W^{KALS}_{\square Si-NaAl}$	14.644 kJ/mol
$\Delta\overline{V}^0_{23}$	0.00000 J/bar	$W^{KALS}_{\square Ca-Na_2}$	0.000 kJ/mol
$\Delta\overline{H}^0_{24}$	42.560 kJ/mol	$W^{KALS}_{\square Na_3Si-K_4Al}$	30.334 kJ/mol
$\Delta\overline{S}^0_{24}$	5.000 J/K-mol	$W^{KALS}_{\square CaNa_2-K_4}$	14.644 kJ/mol
$\Delta\overline{V}^0_{24}$	0.0000 J/bar	$W^{KALS}_{CaAl-NaSi}$	0.000 kJ/mol
$W^{LS}_{H\ Na-K}$	6.862 kJ/mol	W^{LC}_{Na-K}	7.000 kJ/mol
$W^{SS}_{H\ Na-K}$	51.003 kJ/mol	$W^{LC}_{Na,K-H_2O}$	7.000 kJ/mol
$W^{LS}_{V\ Na-K}$	0.33472 J/bar	$\Delta\overline{G}^0_r$	53.000 kJ/mol

kalsilite from experimental determinations of vacancy contents and K/Na ratios of nephelines coexisting with alkali feldspars (Grieg and Barth 1938; Hamilton and MacKenzie 1960; Edgar 1964; Fig. 3, 7) and brackets on 600–1100 °C, K–Na partitioning between aqueous chloride and nepheline solutions and between aqueous chloride solutions and alkali feldspars with disordered Al–Si distributions (Zyrianov et al. 1978; Fig. 7). We then adjust standard state and mixing properties of leucites to be consistent with constraints on subsolidus equilibria involving leucite (Hamilton and MacKenzie 1960; Fudali 1963; Fig. 1). Finally, we calibrate the standard state and mixing parameters for Ca-substituted nephelines and kalsilites based on experimental determinations of nepheline-basic silicate liquid assemblages (Sack et al. 1987a; Gee and Sack 1988; Fig. 1).

Throughout this analysis we make the additional simplifying assumption that all regular-solution-type parameters are positive constants independent of temperature (i.e. $W_G = W_H + P \cdot W_v$). We also adopt the calibrations of Waterwiese et al. (1995) for the standard state properties of low-nepheline, Berman (1988) for the Gibbs energies of albite and K-feldspars, Elkins and Grove (1990) for the mixing parameters of alkali feldspars with disordered Al − Si distributions, and Ghiorso and Sack (1995) for the thermodynamic properties of basic silicate liquids.

Simple system $NaAlSiO_4$–$KAlSiO_4$

Several broad constraints on the thermodynamic parameters of nepheline and kalsilite may be readily deduced under the symmetric approximation, given constraints on miscibility gaps (Ferry and Blencoe 1978) and enthalpy of solution (Hovis and Roux 1993; Fig. 5). First, the strong ordering of K into the large alkali site (LS) in nephelines approximating the $KNa_3Al_4Si_4O_{16}$ composition insures that $W^{SS}_{H\ Na-K}$ cannot be substantially smaller than 66.5 kJ/gfw, an upper bound consistent with the high temperature, nepheline miscibility gap ($T_c \sim 1060$ °C) for the limiting assumption that only K occupies the large alkali site in KNa_3AlSiO_4–$K_4Al_4Si_4O_{16}$ nephelines (i.e. $s = \frac{4}{3}[1 - X_2]$, $X_{2c} = 5/8$). Second, the enthalpies of solution of synthetic nephelines with compositions close to the $NaAlSiO_4$–$KAlSiO_4$ subsystem (Hovis and Roux 1993; Fig. 5), restrict the enthalpy of the reaction

$$\underset{\text{nepheline}}{K_4Al_4Si_4O_{16}} = \underset{\text{kalsilite}}{K_4Al_4Si_4O_{16}}, \tag{25}$$

$\Delta\overline{H}^0_2$, to between about −4 and −8 kJ/gfw, suggest that $W^{LS}_{H\ Na-K} \ll \frac{1}{3} W^{SS}_{H\ Na-K}$, and require that the enthalpies of reactions 9 and 10 ($\Delta\overline{H}^0_{EX}$ and $\Delta\overline{H}^0_X$, respectively) be negative. Third, the entropy of reaction 9, $\Delta\overline{S}^0_{EX}$, must be negative to accommodate both the nepheline miscibility gaps and the enthalpy data (Figs. 2, 5), and the entropy of reaction 10, $\Delta\overline{S}^0_X$, must be positive to produce tetrakalsilite by reaction 1 only above about 800 °C at low pressure (Fig. 7). Fourth, to adjust the $\overline{G}$-X curve of kalsilite at high X_2 to satisfy the temperature-composition systematics of the kalsilite limb of the kalsilite-nepheline miscibility gap (Fig. 2, 6) the entropy of the reaction

$$\underset{\text{nepheline}}{Na_4Al_4Si_4O_{16}} = \underset{\text{kalsilite}}{Na_4Al_4Si_4O_{16}}, \tag{26}$$

$\Delta\overline{S}^0_1$, must be in the range 8.4 –12.6 J/gfw with a metastable reaction temperature between 1400 and 3000 °C ($14 \leq \Delta\overline{H}^0_1 \leq 41$ kJ/gfw) and with W^{KALS}_{Na-K} between

about 6.5 and 7.5 kcal/gfw. Finally, the entropy of reaction 25, $\Delta\overline{S}^0_2$, must be small to negligible to satisfy simultaneously the miscibility gap data and the systematics of the reaction leading to the development of tetrakalsilite at high temperatures and low pressures (Eq. 1).

The essential prerequisite for a viable solution is that it makes explicit provision for the stability of a "tetrakalsilite" molecule approximating the $NaK_3Al_4Si_4O_{16}$ composition at high temperatures and low pressures (cf. Fig. 6a). We have adjusted the appropriate excess entropy and volume terms (e.g., $\Delta\overline{S}^0_{EX}$, $\Delta\overline{S}^0_X$, $\Delta\overline{V}^0_X$, $\Delta\overline{V}^0_{EX}$, $W^{LS}_{V\,Na-K}$, $W^{SS}_{V\,Na-K}$) to ensure that tetrakalsilite appears by reaction 1 at temperatures between 800 and 900 °C at pressures of 0.5 and 2 kbar, but is not stable at 5 kbar and higher pressures (cf. Figs. 2, 6a), an inference consistent with the compositional discontinuities evident in the "kalsilite" limbs of the miscibility gaps observed only at 0.5 and 2 kbar. Solutions which satisfy these constraints are readily achieved providing the discontinuity in nepheline $\overline{V}$-X_2 relations near the $KNa_3Al_4Si_4O_{16}$ composition is due primarily to a negative value of the parameter $\Delta\overline{V}^0_{EX}$ ($= -1.046$ J/bar, Table 3) and $\Delta\overline{V}^0_X$ is negligible (cf. Fig. 4). A negative

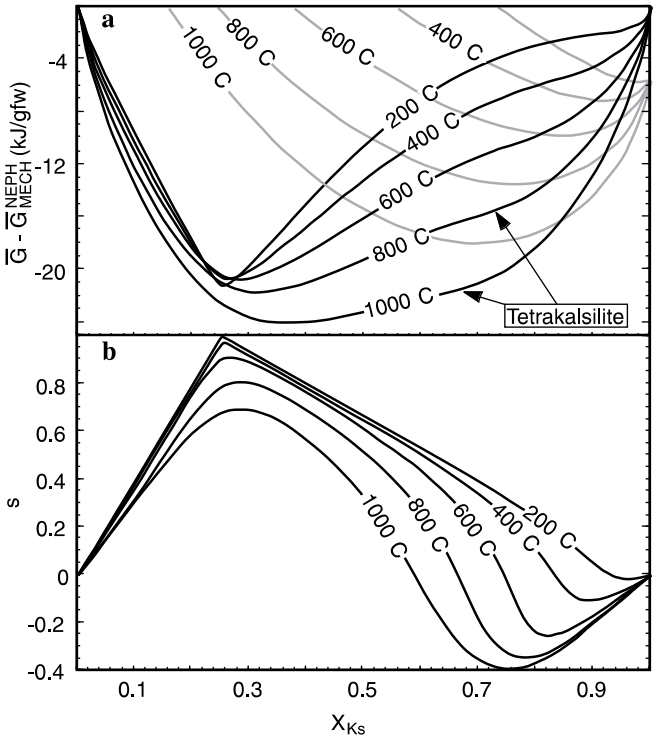

Fig. 6a, b Gibbs energies and values of the order variable s ($X^{LS}_{K^+} - X^{SS}_{K^+}$) for $Na_4Al_4Si_4O_{16} - K_4Al_4Si_4O_{16}$ nephelines and K-rich kalsilites calculated at 200, 400, 600, 800, and 1000 °C and 1 bar. **a** *Solid curves* represent Gibbs energies of mixing of nephelines calculated from Eq. A6a utilizing the parameter values given in Table 3. *Shaded curves* represent the corresponding Gibbs energies of kalsilites relative to those of nephelines calculated from Eq. A6b. **b** Values of the order variable s ($X^{LS}_{K^+} - X^{SS}_{K^+}$) for Na-K nephelines calculated from the condition of homogeneous equilibrium (Eq. 14) simplified for $X_3 = X_4 = 0$ (Eq. A6c)

$\Delta\overline{V}^0_{EX}$ is required to stabilize the $KNa_3Al_4Si_4O_{16}$ molecule relative to the corresponding combination of the $NaK_3Al_4Si_4O_{16}$ molecule and Na- and K-nepheline end-members (reaction 9) with increasing pressure. The apparent magnitude of $\Delta\overline{V}^0_{EX}$ requires that $W^{LS}_{V\,Na-K}$ and $W^{SS}_{V\,Na-K}$ are positive to produce calibrations which satisfy $\overline{V}$-X_2 systematics (Fig. 4) and have a nepheline critical curves displaying permitted dependencies on pressure (Fig. 2). These systematics further bound $\Delta\overline{S}^0_{EX}$ to values slightly more positive than those that would afford values of $\Delta\overline{H}^0_{EX}$ negative enough to be in optimal agreement with enthalpy of solution constraints, because the required values of $\Delta\overline{S}^0_{EX}$ would produce a dP/dT slope for reaction 1, greater than those inferred from the experimental brackets (cf. Fig. 2).

Simple system $NaAlSiO_4$–$KAlSiO_4$–SiO_2

Extension of the calibration for the thermodynamic properties of nephelines into the simple system $NaAlSiO_4$–$KAlSiO_4$–SiO_2 is relatively straightforward. The relevant thermodynamic parameters are constrained by the equilibria governing the following net transport and exchange reactions between alkali feldspars and SiO_2-substituted nephelines:

$$\underset{\text{nepheline}}{Na_4Al_4Si_4O_{16}} + 2\,\underset{\text{alkali feldspar}}{NaAlSi_3O_8} = 2\,\underset{\text{nepheline}}{\square Na_3Al_3Si_5O_{16}} \quad (27)$$

and

$$\frac{1}{4}\underset{\text{nepheline}}{Na_4Al_4Si_4O_{16}} + \underset{\text{alkali feldspar}}{KAlSi_3O_8} = \underset{\text{alkali feldspar}}{NaAlSi_3O_8} + \frac{1}{4}\underset{\text{nepheline}}{K_4Al_4Si_4O_{16}}\,. \quad (28)$$

In light of the experimental data of Grieg and Barth (1938), Edgar (1964), and Hamilton and MacKenzie (1960), the condition of equilibrium for reaction 27 in the $NaAlSiO_4$–SiO_2 subsystem

$$\overline{Q}^*_{\square} \equiv -\Delta\overline{G}^0_{R27} - RT\ln\frac{\left(X^{LS}_{\square}\right)^2}{\left(X^{LS}_{Na^+}\right)} = W_{\square Si-NaAl}\left(X_3^2 - 4X_3 + 2\right) \quad (29)$$

is consistent with the additional simplifying result that $\Delta\overline{H}^0_{R27} \sim \Delta\overline{S}^0_{R27} \sim \Delta\overline{C}p^0_{R27} \sim 0$ and a value of $W_{\square Si-NaAl}$ ($= 14.644$ kJ/gfw, Table 3) producing unmixing in metastable $Na_4Al_4Si_4O_{16}$–$\square Na_3Al_3Si_5O_{16}$ nephelines at 607.7 °C and 1 bar (cf. Fig. 3). This calibration of $\overline{Q}^*_{\square}$ is readily extendible to $(\square_x, K, Na)^{LS}(Na, K)^{SS}_3 Al_{4-x}Si_{4+x}O_{16}$ nephelines, requiring the assumption that mixing in $K_4Al_4Si_4O_{16}$–$\square K_3Al_3Si_5O_{16}$ nephelines ($W_{\square Si-KAl} = 8.368$ kJ/gfw, Table 3) is substantially more ideal than mixing in $Na_4Al_4Si_4O_{16}$–$\square Na_3Al_3Si_5O_{16}$ nephelines to satisfy the experimental data of Hamilton and MacKenzie (1960). Values of $W_{\square Si-KAl}$ inferred from the extended calibration for $\overline{Q}^*_{\square}$ (Fig. 3) are only marginally dependent on the magnitude of $\Delta\overline{G}^0_{23}$, the Gibbs energy of reciprocal reaction between nepheline end-members given by Eq. 11. Assuming $\Delta\overline{S}^0_{23}$ is negligible, $\Delta\overline{G}^0_{23}$ ($= \Delta\overline{H}^0_{23}$) must be at least on the order of 60 kJ/gfw to be consistent with the calorimetric constraints of Hovis and Roux (1993) for nephelines and kalsilites of the natural series ($X_3 \sim 0.21$,

Fig. 5), but its inferred value is marginally dependent on the magnitude of $\Delta\overline{G}^0_{24}$ determined from the subsequent analysis of phase equilibrium in the multisystem. Values of $\Delta\overline{G}^0_{23}$ also fix the estimate for $\Delta\overline{H}^0_f$ of $K_4Al_4Si_4O_{16}$ kalsilite (Table 4) given the condition of equilibrium for reaction 28, $\overline{Q}^*_{K-Na}$ (cf. Fig. 7), the 700 °C nepheline-alkali feldspar tielines determined in the experiments of Hamilton and MacKenzie (1960), and the previously determined constraints on the Gibbs energy of reaction 25. The resulting calibration for $\overline{Q}^*_{K-Na}$ is also compatible with (1) constraints summarized in the subsequent analysis of nepheline equilibrium in the multisystem, and (2) the rather broad constraints on nepheline-alkali feldspar K – Na exchange equilibrium obtained by interpolating between the datasets of Zyrianov et al. (1978) for K – Na exchange between aqueous chloride solutions and nephelines, and between aqueous chloride solutions and alkali feldspars with disordered distributions of Al and Si on tetrahedral sites.

To complete our calibration for $NaAlSiO_4$–$KAlSiO_4$–SiO_2 feldspathoid solutions, we have adjusted the parameters of the model for kalsilite to insure that kalsilites have comparable or lesser equilibrium vacancy contents to nephelines with which they coexist, and we have utilized the experimental constraints on the compositions of coexisting nephelines, alkali feldspars, and leucites of Fudali (1963) and Hamilton and MacKenzie (1960) to render our analysis for the thermodynamic properties of leucite internally consistent with our models for nephelines and kalsilites, and the models of Berman (1988) and Elkins and Grove (1990) for alkali

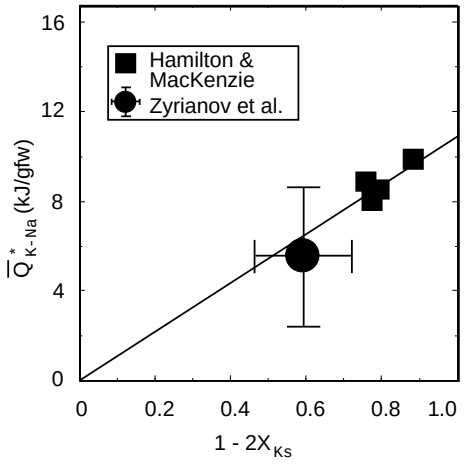

Fig. 7 Calibration of the nepheline-alkali feldspar K-Na exchange reaction (reaction 28) for the simple system $NaAlSiO_4$–$KAlSiO_4$ – SiO_2 (*solid line*), compared with values of $\overline{Q}_{K-Na}$ computed from experimental tielines reported by Hamilton and MacKenzie (1960) (*solid squares*), and the average tieline inferred from the data for K-Na exchange between aqueous chloride solutions and nephelines, and between aqueous chloride solutions and alkali feldspars with disordered Al-Si distributions of Zyrianov et al. (1978) (*circle with attached* 1σ *error bars*). The condition of equilibrium of reaction 28, ($\overline{Q}_{K-Na}$), is expressed as a function of X_2 in zero intercept form with slope $\frac{1}{4}(\Delta\overline{H}^0_X + W^{LS}_{H\,Na-K} + W^{SS}_{H\,Na-K})$, and is given by Eq. A7

felspars. To ensure that kalsilites and nephelines have comparable equilibrium vacancy contents we assign a value to the *vibrational* entropy of the reaction

$$\underset{\text{nepheline}}{\square Na_3Al_3Si_5O_{16}} = \underset{\text{kalsilite}}{\square Na_3Al_3Si_5O_{16}} \tag{30}$$

(cf. Table 4) exactly that required to counterbalance the difference in configurational entropy consequent on the adoption of different reference standard states for these components in nepheline and kalsilite (i.e., $\Delta\overline{S}^{0IC}_{R30} = R[\ln 4 + 3\ln\frac{4}{3}] = 18.7$ J/gfw), and adjust the standard state enthalpy of this reaction to the maximum value permitted by the enthalpy data of Hovis and Roux (1993; Fig. 5) under the simplifying assumptions $W^{KALS}_{\square Na_3Si-K_4Al} = W_{\square Si-KAl} + \frac{3}{4}W^{KALS}_{Na-K}$ and $W^{KALS}_{\square Si-NaAl} = W_{\square Si-NaAl}$.

Multisystem

To extend our calibration to Ca-bearing feldspathoids we have utilized the experimental data of Sack et al. (1987a) and Gee and Sack (1988) in conjunction with the calibration of the thermodynamic properties of natural silicate melts contained with the MELTS software package (Ghiorso and Sack 1995) to analyze statements of nepheline-silicate liquid equilibria. We have adjusted the appropriate parameters of the nepheline and kalsilite models to achieve optimal agreement between nepheline liquidus temperatures and compositions calculated with the MELTS program and their experimental counterparts. As the number of experimental nepheline + natural silicate liquid pairs is quite modest (only 12) and the range in nepheline composition is quite restricted ($X_2 = 0.193 \pm 0.054$, $X_3 = 0.060 \pm 0.067$, $X_4 = 0.324 \pm 0.107$) we have made the assumptions of zero values of the nepheline and kalsilite solution parameters $\Delta\overline{S}^0_{24}$, $W_{\square Ca-Na_2}$, $W_{\square Ca-K_2}$, $W_{CaAl-NaSi}$, $W^{KALS}_{\square Ca-Na_2}$, and $W^{KALS}_{CaAl-NaSi}$, and fixed the remaining kalsilite solution parameters by analogy (i.e., $W^{KALS}_{\square CaNa_2-K_4} = W^{KALS}_{\square Ca-Na_2} + \frac{1}{2}W^{KALS}_{Na-K}$). We have then adjusted values of $\Delta\overline{H}^0_{23}$, $\Delta\overline{H}^0_{24}$, and $\overline{H}^0_f$ of the $\square CaNa_2Al_3Si_5O_{16}$ nepheline end-member (Table 4) to produce optimal agreement between calculated and experimental results for the nepheline + silicate liquid assemblages and for the enthalpy of solution data for the natural series of nephelines and kalsilites of Hovis and Roux (1993; Fig. 5). These adjustments have been integrated into the MELTS software package with the result that the revised MELTS recovers the experimental results for nephelines of Sack et al. (1987a) and Gee and Sack (1988) with mean deviations of -2.73 ± 16.7 °C from the experimental temperatures, and of 0.005 ± 0.031 and 0.002 ± 0.077 for X_2 and X_4. Finally, we have assigned a value of -7.175 J/gfw to the *vibrational* entropy of the reaction

$$\underset{\text{nepheline}}{\square CaNa_2Al_3Si_5O_{16}} = \underset{\text{kalsilite}}{\square CaNa_2Al_3Si_5O_{16}} \tag{31}$$

exactly that required to counterbalance the difference in configurational entropy consequent on the adoption of different reference standard states for these components in nepheline and kalsilite (i.e., $\Delta\bar{S}^{0IC}_{R31} = R[2\ln 8 - 2\ln\frac{9}{2}] = 7.175\,\mathrm{J/gfw}$), and adopted a sufficiently positive value to the standard state enthalpy of reaction 31 (cf. Table 4) to insure that kalsilites are less calcic than the nephelines with which they crystallize in the updated MELTS software.

Standard state properties of cubic $H_2OAlSi_2O_6Na\square_{1/2}$ ($\overline{G}^0_{AN}$) may be obtained from the work of Johnson et al. (1982) who performed adiabatic, solution and drop calorimetric experiments on a natural analcime of composition $H_2OAl_{0.96}Si_{2.04}O_6Na_{0.96}\square_{0.54}$. Their high temperature heat capacity measurements have been adjusted to the stoichiometric composition and fitted to the standard form C_P expression by Berman and Brown (1985). We adopt Berman and Brown's expression and recalculate the preferred values for $\Delta H^0_{f,298}$ and S^0_{298} from Johnson et al. (1982) to conform to stoichiometric analcime: -3308.5 kJ/mol, 232.74 J/mol-K respectively.

Standard state properties for cubic $KAlSi_2O_6\square_{3/2}$ ($\overline{G}^0_{LC}$) are poorly known. Low temperature heat capacities have been measured over the range 53–296 K by Kelley et al. (1953) on a tetragonal sample of presumably "volcanic" leucite from Villa Senni, Italy, whose state of Al-Si order is unknown. These authors estimated an entropy at 298.15 K of 184.1 ± 1.7 J/mol-K. High temperature heat contents of the same sample were measured (over the range 400–1800 K) by Pankratz (1968), who detected a remarkable anomaly in the slope of the heat-content vs T curve near 955 K, but no isothermal absorption of heat accompanying this anomaly. Utilizing the Maier-Kelley type expressions of Pankratz (1968) for the low and high temperature curves on either side of 955 K, and assuming the high temperature measurements refer to the cubic structure, we calculate $\overline{S}^0_{298,cubic} - \overline{S}^0_{298,tetrag}$ of 18.2 J/mol-K, which *suggests* that the "dynamical entropy" (20.66 J/mol-K, see above) may be nearly completely developed by room temperature. It is however, likely that Pankratz's (1968) measurements smooth over the narrow T-interval heat capacity anomalies detected by Lange et al. (1986), to which these authors ascribed an entropy of between 2.4 to 4.3 J/mol-K. If that is the case, then the combined calorimetric measurements of Lange et al. (1986) and Pankratz (1968) account for the "dynamical entropy" contribution to the tetragonal-cubic phase transition. In addition to this entropy, however, there is the entropy associated with $Al - Si$ tetrahedral ordering in tetragonal leucite. The maximum configurational entropy that can be generated from this process is $-3R(\frac{1}{3}\ln\frac{1}{3} + \frac{2}{3}\ln\frac{2}{3})$ or about 15.877 J/mol-K. It is very unlikely that during the course of preparing the calorimetric sample or in the course of performing the experiments, the leucite sample under investigation achieved a state of equilibrium ordering or even deviated substantially from its quenched in, high-T, disordered configuration. Therefore, a "third law" entropy on the order of 22 J/mol-K should probably be added to the value of Kelley et al. (1953) in order to account for both the configurational and residual lattice entropy of disordered tetragonal leucite at room temperature.

As the enthalpy of solution of tetragonal (or cubic) $KAlSi_2O_6\square_{3/2}$ has not been determined, we adopt the following strategy for calculating $\overline{G}^0_{LC}$ as a function of T and P. The parameterization of Berman and Brown (1985) is utilized for the heat capacity measurements of Pankratz (1968) above 298.15 K. In order to account for the "third law" entropy and other entropic effects discussed in the previous paragraph, we increase the value of the entropy at 298.15 K of Kelley et al. (1953) by 21.75 J/mol-K. Then, we obtain an estimate for the enthalpy of formation of the metastable cubic phase at 298.15 K by calibrating a value from experimental data on the compositions of coexisting leucite-ss and silicate melt, internally consistent with adopted values for solution parameters (see below).

Standard state properties for cubic-$NaAlSi_2O_6\square_{3/2}$ ($\overline{G}^0_{Na-LC}$) have not been determined, but heat capacities, entropies and enthalpies of formation of silica-enriched, dehydrated analcime $\square Al_{0.96}Si_{2.04}O_6Na_{0.96}\square_{0.54}$ are tabulated by Johnson et al. (1982). Their high temperature heat capacity measurements have been adjusted to the stoichiometric composition and fitted to the standard form C_P expression by Berman and Brown (1985). We adopt Berman and Brown's expression and recalculate the preferred value S^0_{298} from Johnson et al. (1982) to conform to stoichiometric $\square AlSi_2O_6Na\square_{1/2}$: 173.68 J/mol-K. Next, we assume that the only difference in entropy between $\square AlSi_2O_6Na\square_{1/2}$ and $NaAlSi_2O_6\square_{3/2}$ is configurational and adjust the entropy downward by 7.94 J/K-mol ($-\frac{3}{2}R[\frac{1}{3}\ln\frac{1}{3} + \frac{2}{3}\ln\frac{2}{3}]$) to arrive at an estimate for Na-leucite (165.74 J/K-mol). Then, as with $KAlSi_2O_6\square_{3/2}$, we obtain an estimate for the enthalpy of formation of the metastable cubic phase at 298.15 K by calibrating a value from experimental data on the compositions of coexisting leucite-ss and silicate melt.

By analogy with kalsilite we adopt a value of 7 kJ/mol for W^{LC}_{Na-K}. Utilizing experimental data reported by Ghiorso and Sack (1995) on coexisting compositions of leucite-ss and silicate melt obtained from 1 atmosphere (1050–1300,°C), we calibrate internally consistent values for the enthalpy of formation of cubic $KAlSi_2O_6\square_{3/2}$ and $NaAlSi_2O_6\square_{3/2}$ (Table 4a). Thermodynamic properties for the melt are taken from Ghiorso and Sack (1995), and consequently, the solution properties for leucite-ss reported here are internally consistent with the MELTS model (Ghiorso and Sack 1995). The calibration so obtained exhibits no temperature or compositional dependence to residuals, implying our estimates for the entropies and heat capacities of the anhydrous leucite-ss endmembers are justified. Applying this calibration to the stability of leucite-ss along the binary join $NaAlSi_2O_6$–$KAlSi_2O_6$ results in a maximum Na content of 26 mol% $NaAlSi_2O_6\square_{3/2}$ in leucite-ss at 1050 °C and 1 bar. Fudali (1963) estimated the maximum solubility at

Table 4 Standard State Properties

Table 4a The first line of each entry refers to the heat capacity power function [$C_p = k_0 + k_1 T^{-0.5} + k_2 T^{-2} + k_3 T^{-3}$]. The second line gives properties of phase transitions

C_p (J/K-mol) Phase transition	K_0 $T_{ref}, T\lambda$	$k_1 \times 10^{-2}$	$k_2 \times 10^{-5}$ $\ell_1 \times 10^2$	$k_3 \times 10^{-7}$ $\ell_2 \times 10^5$	[b] ΔH_{tr}
Na_4 Al_4 Si_4O_{16} (neph. and kals.)	820.96	−30.396	−433.532	832.728	
	298., 467.		200.996	633.800	964
$K_4Al_4Si_4O_{16}$ (neph. and kals.)	744.00		−524.268	855.572	
	298., 800.15		−28.286	86.728	4616
□$Na_3Al_3Si_5O_{16}$ (neph. and kals.)[a]	804.12	−39.353	−295.694	523.428	
	298., 467		100.498	331.900	482
□$CaNa_2Al_4Si_4O_{16}$ (neph. and kals.)[a]	849.85	−52.539	−216.766	384.662	
	298., 467		100.498	331.900	482
$KalSi_2O_6$ (leucite)	271.14	−9.441	−78.572	95.920	
	298., 955		−9.731	33.730	256
$NaAlSi_2O_6$ (leucite)	401.27	−42.480		21.630	
$NaAlSi_2O_5(OH)_2$ (leucite)	571.83	−71.887		149.306	

[a] Properties of □$Na_3Al_3Si_5O_{16}$ and □$CaNa_2Al_4Si_4O_{16}$ assumed to be linear combinations of those of $Na_4Al_4Si_4O_{16}$ and high albite, and Na4Al4Si4O_{16} and anorthite (Berman, 1988), respectively.
[b] Coefficients and algorithms from Berman and Brown (1985).

Table 4b 298.15 K entropies, volumes, and enthalpies of formation from the elements

Ref. State	$\Delta\overline{H}^0_f$(kJ/mol)	$\overline{S}^0$(J/K-mol)	$\overline{V}^0$(J/bar-mol)
$Na_4Al_4Si_4O_{16}$ nepheline	–8368.443	497.400	21.6524
$Na_4Al_4Si_4O_{16}$ kalsilite	–8336.297	507.860	21.6524
$K_4Al_4Si_4O_{16}$ nepheline	–8432.606	535.861	24.2157
$K_4Al_4Si_4O_{16}$ kalsilite	–8438.254	535.861	24.1739
□$Na_3Al_3Si_5O_{16}$ nepheline	–8105.840	473.112	21.7367
□$Na_3Al_3Si_5O_{16}$ kalsilite	–8091.196	454.412	21.7367
□$CaNa_2Al_4Si_4O_{16}$ nepheline	–8387.856	448.886	21.7327
□$CaNa_2Al_4Si_4O_{16}$ kalsilite	–8352.672	441.711	21.7327
$KAlSi_2O_6$ (leucite)	–3010.279	205.846	8.8390
$NaAlSi_2O_6$ (leucite)	–3001.976	165.740	8.91
$NaAlSi_2O_5(OH)2$ (leucite)	–3325.900	228.10	9.71

Table 4c Volumetric properties

$V(T,P)$[c]	$v_1 \times 10^6$	$v_2 \times 10^{12}$	$v_3 \times 10^6$	$v_4 \times 10^{10}$
All nephelines and kalsilites	–8.20	20.80	127.208	852.0
All leucites	–1.56	1.27	12.52	0.0

[c] $V(T,P)/V(T_r,P_r) = 1 + v_1 (P-P_r) + v_2 (P-P_r)^2 + v_3(T-T_r) + v_4 (T-T_r)^2$

1 bar and 1000 °C to be about 42 mol%, but his estimate is (presumably ?) extrapolated from higher pressure water saturated experimental runs, and the interpretation of these experiments is problematic.

The remaining solution parameters are estimated by evaluating results from the water-saturated 1 kbar experiments of Fudali (1963) in the system $NaAlSiO_4$–$KAlSiO_4$–SiO_2–H_2O and from petrological studies of the paragenesis of analcime in igneous systems. Fudali (1963) noted that much of the leucite-ss he obtained from quenched hydrothermal runs has a "perthitic" or fine lamellar structure and that the size of the lamellae was related to the rapidity of quench. Optical and X-ray examination of these leucites indicated a lower index of refraction of the lamellar material compared to the host crystal and a correlation of the intensity of the 15.9° 2θ (Cu Kα) peak (indicative of analcime) with the size and abundance of lamellae. Fudali (1963) interpreted these lamellae to be related to exsolution of analcime or sodic-leucite from a more potassic host. The ambiguity in interpretation results from Fudali's (1963) uncertainty regarding the extent to which water is present in leucite-ss under the experimental conditions. This issue of solid solution between leucite and analcime has been the subject of considerable experimental investigation (e.g., Barrer 1982) in regard to the synthesis and hydrothermal chemistry of zeolitic materials. For example, Barrer and Hinds (1953) demonstrated that the extent of solid solution is on the order of 5 mol% at 110°, but these determinations probably bracket limbs of the spinode rather than the binode. Nevertheless, their low-temperature cation exchange experiments argue for substantial solid-solution at more elevated temperatures.

Assuming $W^{LC}_{Na,K-H_2O}$ equals W^{LC}_{Na-K}, then a value of 50 kJ/mol for $\Delta\overline{G}^0_r$ gives a symmetric spinode with limbs

providing about 5% homogeneous solution along the $KAlSi_2O_6\square_{3/2}$–$H_2OAlSi_2O_6Na\square_{1/2}$ (LA) join at 110 °C. The same value puts the solvus limb at $< 0.01\%$ solution. As is obvious from the definition, the parameter $\Delta\overline{G}_r^0$ also determines the stability of $H_2OAlSi_2O_6K\square_{1/2}$ relative to the other end-members. Consequently, $\Delta\overline{G}_r^0$ is the primary model parameter that fixes the Na/K ratio of analcime crystallizing from solution. In order to optimize the value for $\Delta\overline{G}_r^0$, we turn to the work of Luhr and Kyser (1989), who reported the composition of an analcime from a recently erupted minette lava, which they argued represents a primary phenocryst that crystallized under igneous conditions. From the recorded composition of quenched glass associated with this phenocryst (SAY 104, Luhr and Kyser 1989), and the assumption that the analcime crystallized from a (water saturated) liquid of this composition at a pressure of approximately 0.1 GPa, we can assess, using the MELTS algorithm and thermodynamic database (Ghiorso and Sack 1995), the optimal solution parameters that render analcime on the liquidus with the appropriate (measured) Na/K ratio. This exercise gives values of $\Delta\overline{G}_r^0$ equal to $47 + 18 \times \left(T_{\text{liquidus}}\,^\circ\text{C} - 700\right)/300$ kJ/mol and suggests an adjustment to the enthalpy of formation of $H_2OAlSi_2O_6Na\square_{1/2}$ ($\Delta H^0_{f,corr}$) of -9.8–$22.2 \times \left(T_{\text{liquidus}}\,^\circ\text{C} - 700\right)/300$ kJ/mol (Table 4a). Although the latter adjustment is well outside the likely error on the enthalpy reported by Johnson et al. (1982), their value represents a measurement on a non-stoichiometric material. Additionally, the extrapolation of the heat capacity measurements of Johnson et al. (1982) to igneous temperatures is problematic, given the limited temperature range of the measurements (290–623 K) and the tendency for analcime to loose water at elevated temperatures (Helgeson et al. 1978).

Values for $\Delta\overline{G}_r^0$ and $\Delta\overline{H}^0_{f,corr}$ may be further optimized by examining the phase equilibria reported by Fudali (1963). Utilizing the MELTS algorithm (Ghiorso and Sack 1995) to evaluate phase equilibria in the subsystem $KAlSi_2O_6$–$NaAlSi_2O_6$–H_2O we find the best agreement with the 0.1 GPa phase diagram of Fudali (1963) with $\Delta\overline{G}_r^0$ given by 53 kJ/mol and $\Delta\overline{H}^0_{f,corr}$ equal to -17.4 kJ/mol. These adopted values (Tables 3, 4a) generate phase relations that correctly predict the increased Na-content of leucite-ss with falling temperature; up to a maximum of 16 mol% $NaAlSi_2O_6$ at 820 °C where it coexists with both liquid and feldspar ($Or_{0.84}$). At lower temperatures, increased Na-content of leucite-ss causes intersection of the solvus, and phase separation of analcime (An_{96}) accompanies conversion of feldspar to leucite-ss. Subsequent cooling of the system results in destabilization of the analcime in preference to nepheline-ss and feldspar-ss and continued cooling partitions Na from leucite-ss to the other solid phases. Eventually on cooling, leucite-ss is eliminated and replaced by kalsilite-ss. The phase relations calculated using the adopted parameters account for Fudali's (1963) inference of extreme Na-contents of leucite-ss, if these are interpreted as bulk compositions of mixtures of leucite-ss of both the anhydrous and hydrous end-members or perhaps, metastable leucite-ss with compositions interior to the binode but exterior to the spinode. As noted above, optical and X-ray examinations of experimental run products support either of these interpretations (Fudali 1963).

Discussion

Several aspects of our models for feldspathoids merit further, brief discussion, including symmetry of miscibility gap features, development of different nepheline-kalsilite polymorphs from compositions appropriate to K-rich nephelines, and crystallization of feldspathoids from lavas. First, it is apparent that an excellent description of phase equilibrium and calorimetric data may be achieved with a symmetric (i.e., quadratic) non-convergent ordering model for nepheline. In this model tetrakalsilite and nepheline define a structural and chemical continuum at high temperature, with the order parameter serving as a proxy for complex structural changes associated with variations in K/Na ratio. This model makes explicit provision for the well known stability of a $KNa_3Al_4Si_4O_{16}$ component, in which K is strongly ordered into the single large alkali site at low temperatures, and the stability of this ordered vertex of composition-ordering space accounts for the asymmetry of the nepheline-tetrakalsilite miscibility gap with molar $K/(K + Na)$ ratio (note potential analogy with alkali feldspars). The fact that nepheline, tetrakalsilite, trikalsilite, kalsilite, or possibly even sexkalsilite may be developed at room temperature in compositions approximating $NaK_3Al_4Si_4O_{16}$ (e.g., Carpenter and Cellai 1996) reflects quenching history and the strong thermal dependence of the order parameter s in the vicinity of this composition (Fig. 6b), wherein nephelines near the 3/1 K/Na composition exhibit anti-ordering of Na and K between alkali sites (i.e. negative values of the order variable s) at high temperatures but have the expected strong preference for K in the large alkali site (i.e., positive s) at low temperatures. This continuous, high-temperature variability in order parameter is undoubtedly a precondition for development of the various site geometries characteristic of the different nepheline-kalsilite polymorphs at low temperatures. This inference is then consistent with the prediction that the mineral tetrakalsilite ("panunzite" sensu stricto) results from anti-ordering of Na and K between the large cation and the three small cation sites in the nepheline structure (e.g., Hahn and Buerger 1955) at high temperatures. If the predictions of the model are correct, then the anti-ordering of Na and K nephelines displayed at high temperatures constitutes yet another manifestation of the 'fahlore' effect: the systematic dependence of cation ordering on composition displayed prominently in pyroxenes, amphiboles, spinels, and tetrahedrite-tennantite

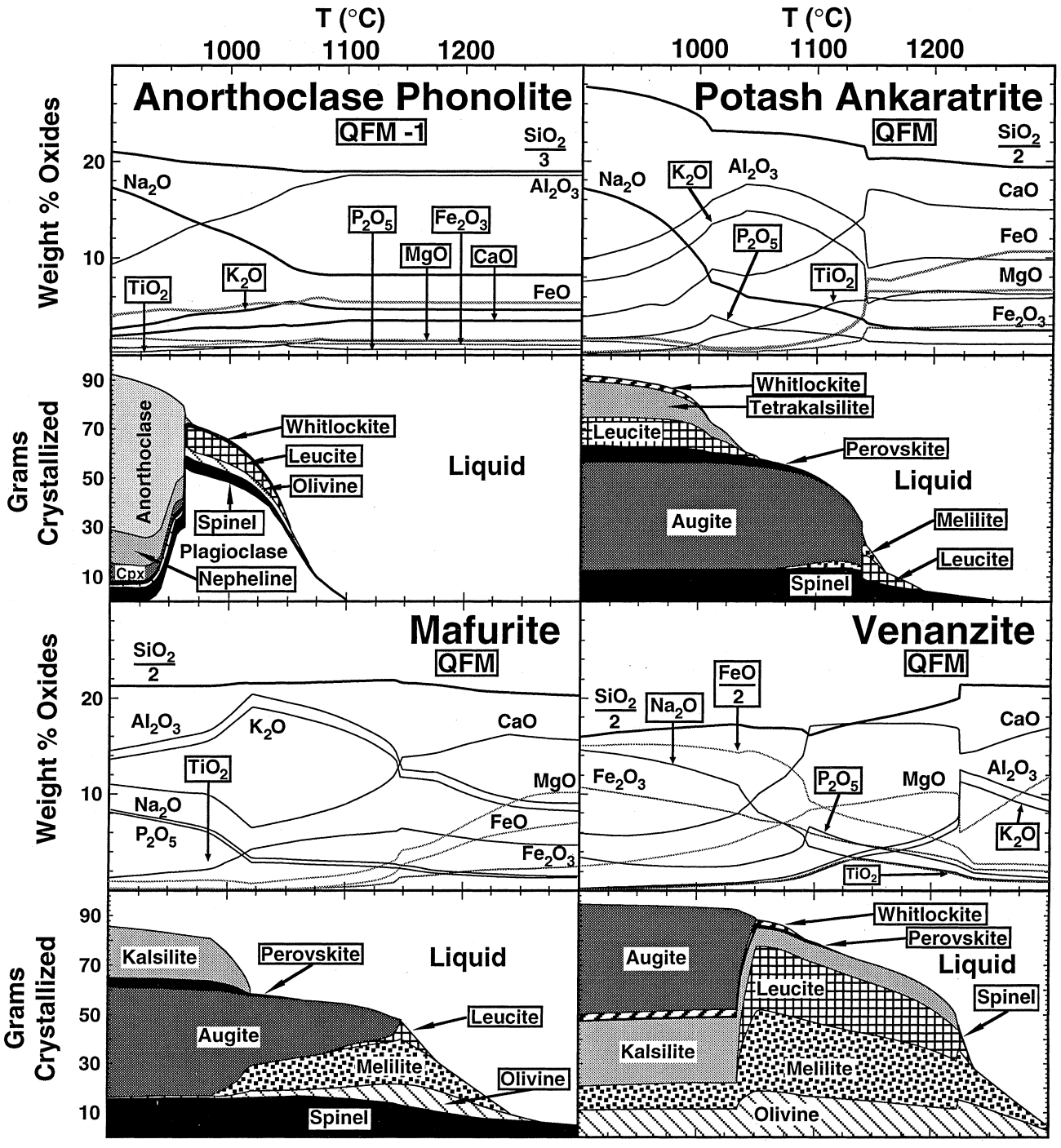

Fig. 8 Equilibrium $SiO_2 - Al_2O_3 - Fe_2O_3 - FeO - MgO - CaO - Na_2O - K_2O - TiO_2 - P_2O_5$ liquids and crystals formed by crystallization of an anorthoclase phonolite (Table 3, #20, Goldich et al. 1975), potash ankaratrite (Brown 1971), mafurite (Table IV, Combe and Holmes 1945), and venanzite (Table I, Bannister et al. 1953) calculated using the MELTS software (Ghiorso and Sack 1995) updated to incorporate the current feldspathoid thermochemical models. The sums of the SiO_2-, Al_2O_3-, Fe_2O_3-, FeO-, MgO-, CaO-, Na_2O-, K_2O-, TiO_2-, and P_2O_5-contents of these rocks analyses have been normalized to 100 wt%, and equilibrium crystallization calculations have been performed on 100 g of initial liquids at oxygen fugacities defined by the QFM buffer (potash ankaratrite, mafurite, and venanzite) and one $\log_{10}$ unit below this buffer (anorthoclase phonolite). In the anorthoclase phonolite, plagioclase, spinel, olivine, leucite, whitlockite, augite, nepheline, and anorthoclase appear at 1102.7, 1075.8, 1070.6, 1053.2, 1045.9, 973.4, and 963.2 °C, and leucite and plagioclase disappear at 962.7 and 942.5 °C. In the potash ankaratrite spinel, leucite, melilite, augite, perovskite, whitlockite, tetrakalsilite, appear at 1262.6, 1195.6, 1162.5, 1144.8, 1116.6, 1141.3, and 1011.8 °C, leucite and melilite disappear at 1141.6 and 1066.6 °C, and leucite reappears at 1059.0 °C. Spinel, olivine, melilite, leucite, augite, perovskite, and kalsilite appear at 1385.5, 1269.5, 1243.5, 1179.1, 1148.4, 1065.0 and 1021.3, and leucite and melilite disappear at 1082.5 and 986.6 °C in mafurite. Olivine, melilite, leucite, spinel, kalsilite, perovskite, whitlockite, and augite appear at 1217.7, 1309.6, 1239.0, 1235.4, 1223.6, 1124.5, 1095.5, and 1052.6 °C, and spinel and leucite disappear at 1223.6 and 1035.4 °C in venanzite

fahlores (e.g., Ghiorso et al. 1995; Robbins et al. 1971; Sack 1992; Sack and Ghiorso 1991b, 1994b).

Using the updated MELTS program we may investigate the crystallization of nephelines, leucites, and kalsilites from lavas to examine the consistency of our models with natural constraints. Here we consider several well characterized silica-poor lavas of varying molar $K_2O/(K_2O + Na_2O)$, K#, and normative SiO_2 content, anorthoclase phonolites from Ross Island in Antarctica, potash ankaratrites and mafurites from the Bunyaruguru volcanic area in south-west Uganda, and venanzites from San Venanzo in Umbria, Italy (Figs. 1, 8). Equilibrium crystallization calculations at, or slightly below, QFM produce the characteristic minerals of these lavas, predicting that all of these lavas crystallize leucite near liquidus temperatures, but only the potash ankaratrite retains leucite at temperatures near its solidus. In the Mn-, Sr-, Ba-, F- and H_2O-free equivalent of the bulk composition of an anorthoclase phonolite reported by Goldich et al. (1975, #20) nepheline ($X_2 = 0.155,\ X_3 = 0.000,\ X_4 = 0.250$) crystallizes at 968.5 °C at QFM -1, about 6 °C above the temperature at which leucite is consumed in a reaction with plagioclase to form alkali feldspar, 962.7 °C, a reaction temperature roughly 115 °C below that determined for the analogous reaction in leucite basanites and minettes (Sack et al. 1987a, Fig. 9). This finding is in accord with petrological observations and the experimental study of Gerke (1995), who determined that nepheline crystallizes at temperatures below 1040 °C. Similar accord characterizes the crystallization calculations for the synthetic equivalent of a potash ankaratrite reported by Brown (1971; Fig. 1). In these calculations (Fig. 8) leucite first crystallizes near the liquidus (Ghiorso and Sack 1995) and is resorbed when augite crystallizes roughly 50 °C lower in temperature. Leucite then reappears approximately 85 °C below its resorption temperature and is joined by nepheline with a tetrakalsilite composition about 10 °C lower in temperature. This tetrakalsilite decomposes to more Na-rich nepheline and kalsilite below 800 °C (Fig. 2) and this decomposition could produce the complex intergrowths of nepheline and kalsilite observed in the groundmass (Combe and Holmes 1945; Brown 1971). In accordance with its higher K# and lower normative SiO_2, the synthetic equivalent of the mafurite composition from Combe and Holmes (1945; Fig. 1) crystallizes kalsilite before tetrakalsilite at 1021.3 °C, and is saturated with leucite only over a 66 °C interval ending 61 °C above the temperature of initial kalsilite crystallization. Finally, the synthetic equivalent of the leucite- and kalsilite-bearing venanzite reported by Bannister et al. (1953) is saturated with nearly K-end-member kalsilites and leucites over a 189 °C interval (1224–1035 °C) terminated by the crystallization of augite. With resorption of leucite (i.e., removal of the silica buffer defined by the coexistence of kalsilite and leucite), residual venanzite liquids become spectacularly enriched in FeO and Fe_2O_3, and also exhibit the pronounced Na_2O-enrichments seen in anorthoclase phonolite, potash ankaratrite, and mafurite residual liquids (Fig. 8).

Acknowledgements We gratefully acknowledge material support for this investigation provided by the National Science Foundation through grants EAR91-04714 (MSG) and EAR92-19083 (ROS) and the constructive reviews of Richard N. Abbott (RNA) and Michael Carpenter.

Appendix

Expressions for calculating curves in Figures 3–7

Fig. 3

$$\begin{aligned}\overline{Q}^{*}_{\square} \equiv & -\Delta\overline{G}^{0}_{R27} - RT\ln\frac{(X^{LS}_{\square})^2(X^{SS}_{Na^+})^3}{(X^{LS}_{Na^+})(a^{AF}_{NaAlSi_3O_8})^2} \\ & - \left[\Delta\overline{G}^{0}_{X} + W^{LS}_{Na-K} + W^{SS}_{Na-K}\right](X_2)^2 \\ & + \frac{1}{16}\left[3\,\Delta\overline{G}^{0}_{X} - 9\,W^{LS}_{Na-K} - W^{SS}_{Na-K}\right](s^2) \\ & - \frac{1}{2}\left[\Delta\overline{G}^{0}_{X} + 3\,W^{LS}_{Na-K} - W^{SS}_{Na-K}\right](X_2)(s) \\ & - \frac{1}{2}\left[2\,\Delta\overline{G}^{0}_{23} + \Delta\overline{G}^{0}_{EX} - \Delta\overline{G}^{0}_{X} - 2\,W^{LS}_{Na-K}\right. \\ & \left. - 2\,W_{\square Si-NaAl} + 2\,W_{\square Si-KAl}\right](X_2)(2 - X_3) \\ & - \frac{1}{8}\left[\Delta\overline{G}^{0}_{X} - \Delta\overline{G}^{0}_{EX} - 2\,\Delta\overline{G}^{0}_{23} - 6\,W^{LS}_{Na-K}\right. \\ & \left. - 6\,W_{\square Si-NaAl} + 6\,W_{\square Si-KAl}\right](2 - X_3)(s) \\ = & W_{\square Si-NaAl}(X_3^2 - 4X_3 + 2). \end{aligned} \tag{A3}$$

Albite activity in alkali feldspar ($a^{AF}_{NaAlSi_3O_8}$) calculated from algorithms given by Elkins and Grove (1990), alkali feldspars are assumed to have disordered Al—Si distributions, and $\Delta\overline{H}^{0}_{R27} = 0.00$ kJ/gfw, $\Delta\overline{S}^{0}_{R27} = 0.00$ J/gfw, and $\Delta\overline{V}^{0}_{R27} = 1.655$ J/bar (cf. Tables 3, 4; Berman, 1988).

Fig. 4

$$\begin{aligned}\overline{V}_{Neph} = & \ \overline{V}^{0}_{1\,Neph}(1 - X_2 - X_3 - X_4) + (\overline{V}^{0}_{2\,Kals} - \Delta\overline{V}^{0}_{2})(X_2) \\ & + \overline{V}^{0}_{3\,Neph}(X_3) \ + \overline{V}^{0}_{4\,Neph}(X_4) + \\ & \frac{1}{4}\left[2\,\Delta\overline{V}^{0}_{EX} + \Delta\overline{V}^{0}_{X} + 3\,W^{LS}_{V\,Na-K} - W^{SS}_{V\,Na-K}\right](s) \\ & + \left[\Delta\overline{V}^{0}_{X} + W^{LS}_{V\,Na-K} + W^{SS}_{V\,Na-K}\right](X_2)(1 - X_2) \\ & + \frac{1}{16}\left[3\,\Delta\overline{V}^{0}_{X} - 9\,W^{LS}_{V\,Na-K} - W^{SS}_{V\,Na-K}\right](s^2) \\ & - \frac{1}{2}\left[\Delta\overline{V}^{0}_{X} + 3\,W^{LS}_{V\,Na-K} - W^{SS}_{V\,Na-K}\right](X_2)(s) \\ & + \frac{1}{2}\left[2\,\Delta\overline{V}^{0}_{23} + \Delta\overline{V}^{0}_{EX} - \Delta\overline{V}^{0}_{X} - 2\,W^{LS}_{V\,Na-K}\right](X_2)(X_3) \\ & + \frac{1}{8}\left[\Delta\overline{V}^{0}_{X} - \Delta\overline{V}^{0}_{EX} - 2\,\Delta\overline{V}^{0}_{23} - 6\,W^{LS}_{V\,Na-K}\right](X_3)(s) \\ & + \frac{1}{3}\left[3\,\Delta\overline{V}^{0}_{24} + \Delta\overline{V}^{0}_{EX} - 2\,\Delta\overline{V}^{0}_{X}\right. \\ & \left. - 3\,W^{LS}_{V\,Na-K} - W^{SS}_{V\,Na-K}\right](X_2)(X_4) \\ & + \frac{1}{12}\left[-9\,W^{LS}_{V\,Na-K} + W^{SS}_{V\,Na-K} - 3\,\Delta\overline{V}^{0}_{EX} - 9\,\Delta\overline{V}^{0}_{24}\right](X_4)(s) \end{aligned} \tag{A4a}$$

for $(0 < X_2 < 0.73)$ and

$$\overline{V}_{Kals} = (\overline{V}^0_{1\,Neph} + \Delta\overline{V}^0_1)(1 - X_2 - X_3 - X_4) + \overline{V}^0_{2\,Kals}(X_2) + (\overline{V}^0_{3\,Neph} + \Delta\overline{V}^0_3)(X_3) + (\overline{V}^0_{4\,Neph} + \Delta\overline{V}^0_4)(X_4) \quad \text{(A4b)}$$

for $(0.73 < X_2 < 1.00)$, utilizing parameter values given in Tables 3 and 4 and values of s computed at 200 °C

Fig.5

m

$$\begin{aligned}\overline{H}^{Soln}_{Neph} = {} & \overline{H}^{Soln}_{1\,Neph}(1 - X_2 - X_3 - X_4) + \left[\overline{H}^{Soln}_{2\,Kals} - \frac{1}{4}\Delta\overline{H}^0_2\right](X_2) \\ & + \overline{H}^{Soln}_{3\,Neph}(X_3) + \overline{H}^{Soln}_{4\,Neph}(X_4) \\ & + \frac{1}{4}\left[\frac{1}{4}\left[2\,\Delta\overline{H}^0_{EX} + \Delta\overline{H}^0_X + 3\,W^{LS}_{H\,Na-K} - W^{SS}_{H\,Na-K}\right](s)\right. \\ & \left. + \left[\Delta\overline{H}^0_X + W^{LS}_{H\,Na-K} + W^{SS}_{H\,Na-K}\right](X_2)(1 - X_2)\right. \\ & + \frac{1}{16}\left[3\,\Delta\overline{H}^0_X - 9\,W^{LS}_{H\,Na-K} - W^{SS}_{H\,Na-K}\right](s^2) \\ & - \frac{1}{2}\left[\Delta\overline{H}^0_X + 3\,W^{LS}_{H\,Na-K} - W^{SS}_{H\,Na-K}\right](X_2)(s) \\ & + W_{\square Si-NaAl}(X_3)(1 - X_3) \\ & + \frac{1}{2}\left[2\,\Delta\overline{H}^0_{23} + \Delta\overline{H}^0_{EX} - \Delta\overline{H}^0_X - 2\,W^{LS}_{H\,Na-K}\right. \\ & \left. - 2\,W_{\square Si-NaAl} + 2\,W_{\square Si-KAl}\right](X_2)(X_3) \\ & + \frac{1}{8}\left[\Delta\overline{H}^0_X - \Delta\overline{H}^0_{EX} - 2\,\Delta\overline{H}^0_{23} - 6\,W^{LS}_{H\,Na-K}\right. \\ & \left. - 6\,W_{\square Si-NaAl} + 6\,W_{\square Si-KAl}\right](X_3)(s) \\ & + W_{\square Ca-Na_2}(X_4)(1 - X_4) \\ & + \frac{1}{3}\left[3\,\Delta\overline{H}^0_{24} + \Delta\overline{H}^0_{EX} - 2\,\Delta\overline{H}^0_X - 3\,W^{LS}_{H\,Na-K}\right. \\ & \left. - W^{SS}_{H\,Na-K} + 3\,W_{\square Ca-K_2} - 3\,W_{\square Ca-Na_2}\right](X_2)(X_4) \\ & + (W_{CaAl-NaSi} - W_{\square Ca-Na_2} - W_{\square Si-NaAl})(X_3)(X_4) \\ & + \frac{1}{12}\left[9\,W_{\square Ca-K_2} - 9\,W_{\square Ca-Na_2} - 9\,W^{LS}_{H\,Na-K} + W^{SS}_{H\,Na-K}\right. \\ & \left. \left. - 3\Delta\overline{H}^0_{EX} - 9\,\Delta\overline{H}^0_{24}\right](X_4)(s)\right] \end{aligned} \quad \text{(A5a)}$$

for $(0 < X_2 < 0.73)$ and

$$\begin{aligned}\overline{H}^{Soln}_{Kals} = {} & \left[\overline{H}^{Soln}_{1\,Neph} + \frac{1}{4}\Delta\overline{H}^0_1\right](1 - X_2 - X_3 - X_4) + \overline{H}^{Soln}_{2\,Kals}(X_2) \\ & + \left[\overline{H}^{Soln}_{3\,Neph} + \frac{1}{4}\Delta\overline{H}^0_3\right](X_3) + \left[\overline{H}^{Soln}_{4\,Neph} + \frac{1}{4}\Delta\overline{H}^0_4\right](X_4) \\ & + \frac{1}{4}\left[W^{KALS}_{Na-K}(1 - X_2)(X_2) + W^{KALS}_{\square Si-NaAl}(1 - X_3)(X_3)\right. \\ & + W^{KALS}_{\square Ca-Na_2}(1 - X_4)(X_4) \\ & + (W^{KALS}_{\square Na_3Si-K_2Al} - W^{KALS}_{\square Si-NaAl} - W^{KALS}_{Na-K})(X_2)(X_3) \\ & + (W^{KALS}_{\square CaNa_2-K_4} - W^{KALS}_{\square Ca-Na_2} - W^{KALS}_{Na-K})(X_2)(X_4) \\ & + (W^{KALS}_{CaAl-NaSi} - W^{KALS}_{\square Ca-Na_2} \\ & \left. - W^{KALS}_{\square Si-NaAl})(X_3)(X_4)\right] \end{aligned} \quad \text{(A5b)}$$

for $(0.73 < X_2 \leq .985)$, $\overline{H}^{Soln}_{1\,Neph} = 89.515$, $\overline{H}^{Soln}_{2\,Kals} = 85.85$, $\overline{H}^{Soln}_{3\,Neph} = 85.4$, and $\overline{H}^{Soln}_{4\,Neph} = 84.2$, kcal/gfw, and values of s computed at 200°C.

Fig.6

$$\begin{aligned}\overline{G} - \overline{G}^{NEPH}_{MECH} = {} & + \frac{1}{4}\left[2\,\overline{G}^0_{EX} + \Delta\overline{G}^0_X + 3\,W^{LS}_{Na-K}W^{SS}_{Na-K}\right](s) \\ & + \left[\Delta\overline{G}^0_X + W^{LS}_{Na-K} + W^{SS}_{Na-K}\right](X_2)(1 - X_2) \\ & + \frac{1}{16}\left[3\,\Delta\overline{G}^0_X - 9\,W^{LS}_{Na-K} - W^{SS}_{Na-K}\right](s^2) \\ & - \frac{1}{2}(\Delta\overline{G}^0_X + 3\,W^{LS}_{Na-K} - W^{SS}_{Na-K})(X_2)(s) \\ & + RT\left\{\left[X_2 + \frac{3}{4}s\right]\ln\left\{X_2 + \frac{3}{4}s\right\} + \left(1 - X_2 - \frac{3}{4}s\right)\right. \\ & \ln\left\{1 - X_2 - \frac{3}{4}s\right\} + 3\left(X_2 - \frac{1}{4}s\right)\ln\left\{X_2 - \frac{1}{4}s\right\} \\ & \left. + 3\left(1 - X_2 + \frac{1}{4}s\right)\ln\left\{1 - X_2 + \frac{1}{4}s\right\}\right. \end{aligned} \quad \text{(A6a)}$$

$$\left[\overline{G}^{NEPH}_{MECH} = \overline{G}^{0\,NEPH}_{Na_4Al_4Si_4O_{16}}(1 - X_2) - \overline{G}^{0\,NEPH}_{K_4Al_4Si_4O_{16}}(X_2)\right],$$

$$\begin{aligned}\overline{G} - \overline{G}^{NEPH}_{MECH} = {} & \Delta\overline{G}^0_1(1 - X_2) + \Delta\overline{G}^0_2(X_2) + W^{KS}_{Na-K}(1 - X_2)(X_2) \\ & + 4\,RT\{[X_2]\ln\{X_2\} + (1 - X_2)\ln\{1 - X_2\}\} \end{aligned} \quad \text{(A6b)}$$

where $\Delta\overline{G}^0_1 = (\overline{G}^{0\,KALS}_{Na_4Al_4Si_4O_{16}} - \overline{G}^{0\,NEPH}_{Na_4Al_4Si_4O_{16}})$ and $\Delta\overline{G}^0_2 = (\overline{G}^{0\,KALS}_{K_4Al_4Si_4O_{16}} - \overline{G}^{0\,NEPH}_{K_4Al_4Si_4O_{16}})$, and the condition of homogeneous equilibrium for $(Na,K)_4Al_4Si_4O_{16}$ nephelines

$$\begin{aligned} & RT\ln\left[\left(\frac{X^{LS}_{Na^+}}{X^{LS}_{K^+}}\right)\left(\frac{X^{SS}_{K^+}}{X^{SS}_{Na^+}}\right)\right] \\ & = \frac{2}{3}\Delta\overline{G}^0_{EX} \\ & + \frac{1}{6}\left[3\,\Delta\overline{G}^0_X - 9\,W^{LS}_{Na-K} - W^{SS}_{Na-K}\right](s) \\ & + \frac{1}{3}\left[\Delta\overline{G}^0_X + 3\,W^{LS}_{Na-K} - W^{SS}_{Na-K}\right](1 - 2\,X_2). \end{aligned} \quad \text{(A6c)}$$

Fig.7

$$\begin{aligned}\overline{Q}^*_{K-Na} \equiv {} & -\Delta\overline{G}^0_{R28} - \frac{1}{4}RT\ln\frac{(a^{AF}_{NaAlSi_3O_8})^4(X^{LS}_{K^+})(X^{SS}_{K^+})^3}{(a^{AF}_{KAlSi_3O_8})^4(X^{LS}_{Na^+})(X^{SS}_{Na^+})^3} \\ & + \frac{1}{8}\left[\Delta\overline{G}^0_X + 3\,W^{LS}_{Na-K} - W^{SS}_{Na-K}\right](s) \\ & - \frac{1}{8}\left[2\,\Delta\overline{G}^0_{23} + \Delta\overline{G}^0_{EX} - \Delta\overline{G}^0_X - 2\,W^{LS}_{Na-K}\right. \\ & \left. - 2\,W_{\square Si-NaAl} + 2\,W_{\square Si-KAl}\right](X_3) \\ & - \frac{1}{4}\left[-T\,\Delta\overline{S}^0_X + (P - 1)\left(\Delta\overline{V}^0_X + W^{LS}_{V\,Na-K} + W^{SS}_{V\,Na-K}\right)\right] \\ & \times (1 - 2\ X_2) \\ = {} & + \frac{1}{4}\left[\Delta\overline{H}^0_X + W^{LS}_{H\,Na-K} + W^{SS}_{H\,Na-K}\right](1 - 2\,X_2), \end{aligned}$$

where $\Delta\overline{G}^0_{R28}$ is the Gibbs energy of reaction 28 defined from the values for Gibbs energies of albites and sanadines with disordered Al–Si distributions given by Berman (1988) and the Gibbs energies of Na- and K-nephelines given in Table 4, and $a^{AF}_{NaAlSi_3O_8}$ and $a^{AF}_{KAlSi_3O_8}$ are defined from the expressions given by Elkins and Grove (1990).

References

Abbott RN Jr (1984) $KalSiO_4$ stuffed derivatives of tridymite: phase relationships. Am Mineral 69: 449–457

Andou Y, Kawahara A (1982) The existence of high-low inversion point of kalsilite. Mineral J 11: 72–77

Bannister FA, Hey MH (1931) A chemical, optical and X-ray study of nepheline and kaliophilite. Mineral Mag 22: 569–608

Bannister FA, Sahama THG, Wiik HB (1953) Kalsilite in venanzite from San Venanzo, Umbria, Italy. Mineral Mag 30: 46–48

Barrer RM (1982) Hydrothermal chemistry of zeolites. Academic Press, New York

Barrer RM, Hinds L (1953) Ion-exchange in crystals of analcite and leucite. J Chem Soc xx: 1879–1888

Barth TF (1963) The composition of nepheline. Schweiz Mineral Petrogr Mitt 43: 153–164

Berman RG (1988) Internally-consistent thermodynamic data for minerals in the system Na_2O–K_2O– CaO–MgO–FeO–Fe_2O_3 – Al_2O_3–SiO_2–TiO_2–H_2O—CO_2. J Petrol 29: 445–522

Berman RG, Brown TH (1985) Heat capacities of minerals in the system Na_2O–K_2O–CaO–MgO–FeO–Fe_2O_3–Al_2O_3–SiO_2–TiO_2–H_2O–CO_2: representation, estimation, and high temperature extrapolation. Contrib Mineral Petrol 89: 168–183

Bonaccorsi E, Merlino S, Pasero M (1988) Trikalsilite: its structural relationships with nepheline and tetrakalsilite. N Jahrb Mineral Monatstin: 559–567

Bowen NL (1912) The binary system: $Na_2Al_2Si_2O_8$ (nepheline, carnegieite)–$CaAl_2Si_2O_8$ (anorthite). Am J Sci 33: 551–573

Boysen H (1990) Neutron scattering and phase transitions in laucite. In: Salje EKH (ed) Phase transitions in ferroelastic and co-elastic crystals. Cambridge University Press, New York, 334–49

Brown FH (1971) Volcanic petrology of recent volcanic rocks in the Lake Rudolf region, Kenya. Unpublished PhD thesis, University of California, Berkeley

Buerger MJ, Klein GE, Donnay G (1954) Determination of the crystal structure of nepheline. Am Mineral 39: 805–818

Carpenter MA, Cellai D (1996) Microstructures and high-temperature phase transitions in kalsilite. AmMineral 81: 561–584

Cellai D, Carpenter MA, Heaney PJ (1992) Phase transitions and microstructures in natural kaliophilite. Eur J Mineral 4: 1209–1220

Combe AD, Holmes A (1945) The kalsilite-bearing lavas of Kabirenge and Lyakauli, South-West Uganda. Trans R Soc Edinb 61: 359–380

Darken LS, Gurry RW (1953) Physical Chemistry of Metals. McGraw-Hill, New York

Deer WA, Howie RA, Zussman J (1963) Rock forming minerals (vol. 4 Framework silicates). Wiley, New York

Dollase, WA, Freeborn WP (1977) The structure of $KAlSiO_4$ with $P6_3mc$ symmetry. Am Mineral 62: 336–340

Dollase WA, Thomas WA (1978) The crystal chemistry of silica-rich, alkali-deficient nepheline. Contrib Mineral Petrol 66: 311–318

Donnay G, Schairer JF, Donnay JDH (1959) Nepheline solid solutions. Mineral Mag 32: 93–109

Edgar AD (1964) Phase-equilibrium relations in the system nepheline-albite-water at 1,000 kg/cm^2. J Geol 72: 448–460

Elkins LT, Grove TL (1990) Ternary feldspar experiments and thermodynamic models. Am Mineral 75: 544–559

Ferry JM, Blencoe JG (1978) Subsolidus phase relations in the nepheline-kalsilite system at 0.5, 2.0, and 5.0 kbar. Am Mineral 63: 1225–1240

Fudali RF (1963) Experimental studies bearing on the origin of pseudoleucite and associated problems of alkalic rock systems. Geol Soc Am Bull 74: 1101–1126

Fuhrman ML, Lindsley DH (1988) Ternary feldspar modeling and thermometry. Am Mineral 73: 201–215

Gee LL, Sack RO (1988) Experimental petrology of melilite nephelinites. J Petrol 29: 1233–1255

Gerke TL (1995) Low pressure experiments with basanite, hawaiite, and phonolite from Mt. Erebus, Antarctica. PhD thesis. University of Cincinnati

Ghiorso MS (1984) Activity/composition relations in the ternary feldspars. Contrib Mineral Petrol 87: 282–296

Ghiorso MS (1990a) Thermodynamic properties of hematite-ilmenite-geikielite solid solutions. Contrib Mineral Petrol 104: 645–667

Ghiorso MS (1990b) The application of the Darken equation to mineral solid solutions with variable degrees of order-disorder. Am Mineral 75: 539–543

Ghiorso MS, Sack RO (1991) Fe-Ti oxide geothermometry: thermodynamic formulation and the estimation of intensive variables in silicic magmas. Contrib Mineral Petrol 108: 485–510

Ghiorso MS, Sack RO (1995) Chemical mass transfer in magmatic processes IV. A revised and internally consistent thermodynamic model for the interpolation and extrapolation of liquid-solid equlibrium in magmatic systems at elevated temperatures and pressures. Contrib Mineral Petrol 119: 197–212

Ghiorso MS, Carmichael ISE, Moret LK (1979) Inverted high-temperature quartz. Unit cell parameters and properties of the alpha-beta inversion. Contrib Mineral Petrol 68: 307–28

Ghiorso MS, Evans BW, Hirchmann MM, Yang H (1995) Thermodynamics of the amphiboles: Fe-Mg cummingtonite solid solutions. Am Mineral 80: 502–519

Goldich SS, Treves SB, Suhr NH, Stuckless JS (1975) Geochemistry of the Cenozoic rocks of Ross Island and vicinity, Antartica. J Geol 83: 415–435

Gregorkiewitz M, Shäfer H (1980) The structure of $KAlSiO_4$-kaliophilite O1: application of the subgroup-supergroup relations to the quantitative space group determination of pseudosymmetric crystals. Sixth European Crystallograph Meeting, Barcelona. Abstracts with Program, p 155

Grieg JW, Barth TF (1938) The system $Na_2O \cdot Al_2O_3 \cdot 2SiO_2$ (Nepheline, carnegieite) – $Na_2O \cdot Al_2O_3 \cdot 6SiO_2$ (Albite). Am J Sci 35A: 93–112

Hahn T, Buerger MJ (1955) The detailed structure of nepheline, $KNa_3Al_4Si_4O_{16}$. Z Kristallogr 106: 308–338

Hamilton DL, MacKenzie WS (1960) Nepheline solid solution in the system $NaAlSiO_4$—$KAlSiO_4$—SiO_2. J Petrol 1: 56–72

Hamilton DL, MacKenzie WS (1961) Nephelines as crystallization temperature indicators. J Geol 69: 321–329

Haselton HT Jr, Hovis GL, Hemingway BS, Robie RA (1983) Calorimetric investigation of the excess entropy of analbite-sanadine solid solutions: lack of evidence for Na, K short-range order and implications for two-feldspar thermometry. Am Mineral 68: 398–413

Hatch DM, Ghose S, Stokes HT (1990) Phase transitions in leucite, $KAlSi_2O_6$. I. Symmetry analysis with order parameter treatment and the resulting microscopic distortions. Phys Chem Mineral 17: 220–227

Helgeson HC, Delany JM, Nesbit HW, Bird DK (1978) Summary and critique of the thermodynamic properties of the common rock-forming minerals. Am J Sci 278A: 1–299

Hirschmann M (1991) Thermodynamics of multicomponents olivines and the solution properties of $(Ni,Mg,Fe)_2SiO_4$ and $(Ca,Mg,Fe)_2SiO_4$ olivines. Am Mineral 76: 1232–1248

Hovis GL, Roux J (1993) Thermodynamic mixing properties of nepheline-kalsilite crystalline solutions. Am J Sci, 293: 1108–1127

Hovis GL, Delbove F, Bose RB (1991) Gibbs energies and entropies of K-Na mixing for alkali feldspars from phase equilibrium data: implication for feldspar solvi and short-range order. Am Mineral 76: 913–927

Hovis GL, Spearing DR, Stebbins JF, Roux J, Clare A (1992) X-ray powder diffraction and ^{23}Na, ^{27}Al, and ^{29}Si MAS-NMR investigation of nepheline-kalsilite crystalline solutions. Am Mineral 77: 19–29

Johannsen A (1938) A descriptive petrography of the igneous rocks. Volume IV. Part I: the feldspathoid rocks. University of Chicago Press, Chicago Illinois

Johnson GK, Flotow HE, O'Hare AG, Wise WS (1982) Thermodynamic studies of zeolites: analcime and dehydrated analcime. Am Mineral 67: 736–748

Kawahara A, Andou Y, Marumo F, Okuno M (1987) The crystal structure of high temperature form of kalsilite ($KalSiO_4$) at 950°C. Mineral J 11: 260–270

Kelley KK, Todd SS, Orr RL, King EG, Bonnickson KR (1953) Thermodynamic properties of sodium-aluminum and potassium-aluminum silicates. US Bur Mines Rep Invest 4955

Lange RA, Carmichael ISE, Stebbins JF (1986) Phase transitions in leucite ($KalSi_2O_6$), orthorhombic $KalSiO_4$, and their iron analogues ($KfeSi_2O_6$, $KfeSiO_4$). Am Mineral 71: 937–45

Luhr JF, Kyser TK (1989) Primary igneous analcime: the colima minettes. Am Mineral 74: 216–23

Luth WC, Fenn PM (1973) Calculation of binary solvii with special reference to the sanidine-high albite solvus. Am Mineral 58: 1009–15

Mazzi F, Galli E, Gottardi G (1976) The crystal structure of tetragonal leucite. Am Mineral 61: 108–115

Merlino S (1984) Feldspathoids: their average and real structures. In: Brown WL (ed): Feldspars and feldspathoids (NATO ASI ser C, vol. 137). Reidel, Dordrecht, pp 435–470

Merlino S, Franco E, Mattia CA, Pasero M, De Gennaro M (1985) The crystal structure on panunzite (natural tetrakalsilite). N Jahrb Mineral Monats: 322–328

Palmer DC (1990) Volume anomaly and the impure ferroelastic phase transition in leucite. In: Salje EKH (ed) Phase transitions in ferroelastic and co-elastic crystals. Cambridge University Press, New York, pp 350–66

Palmer DC (1994) Stuffed derivatives of the silica polymorphs. In: Heany PJ, Prewitt CT, Gibbs GV (eds) Silica: physical behavior, geochemistry and materials applications (Reviews in Mineralogy vol. 29). Mineralogical Society of America, Washington DC, pp 83–122

Palmer DC, Salje EKH (1990) Phase transitions in leucite: dielectric properties and transition mechanism. Phys Chem Mineral 17: 444–452

Palmer DC, Putnis A, Salje EKH (1988) Twinning in tetragonal leucite. Phys Chem Mineral 16: 298–303

Palmer DC, Salje EKH, Schmahl WW (1989) Phase transitions in leucite: X-ray diffraction studies. Phys Chem Mineral 16: 714–719

Palmer DC, Bismayer U, Salje EKH (1990) Phase transitions in leucite: order parameter behavior and the Landau potential deduced from Raman spectroscopy and birefringence studies. Phys Chem Mineral 17: 259–65

Pankratz LB (1968) High-temperature heat contents and entropies of dehydrated analcite, kaliophilite, and leucite. US Bur Mines Rep Invest 7073

Peacor DR (1968) A high temperature single crystal diffractometer study of leucite, $(K,Na)AlSi_2O_6$. Z Kristallogr 127: 213–24

Perrota AJ, Smith JV (1965) the crystal structure of kalsilite, $KalSiO_4$. Mineral Mag 35: 588–595

Robbins M, Wertheim GK, Sherwood RC, Buchanan DNE (1971) Magnetic properties and site distributions in the system $FeCr_2O_4Fe_3O_4$ ($Fe^{2+}Cr_{2-x}Fe_x^{3+}O_4$). J Phys Chem Solids 32: 717–729

Roux J, Hamilton DL (1976) Primary igneous analcite – an experimental study. J Petrol 17: 244–57

Sack RO (1982) Spinels as petrogenetic indicators: activity-composition relations at low pressures. Contrib Mineral Petrol 79: 169–186

Sack RO, Ghiorso MS (1989) Importance of considerations of mixing properties in establishing an internally consistent thermodynamic database: thermochemistry of minerals in the system Mg_2SiO_4–Fe_2SiO_4–SiO_2. Contrib Mineral Petrol 102: 41–68

Sack RO, Ghiorso MS (1991a) An internally consistent model for the thermodynamic properties of Fe-Mg-titanomagnetite-aluminate spinels. Contrib Mineral Petrol 106: 474–505

Sack RO Ghiorso MS (1991b) Chromian spinels as petrogenetic indicators: thermodynamics and petrological applications. Am Mineral 76: 827–847

Sack RO, Ghiorso MS (1994a) Thermodynamics of multicomponent pyroxenes. I. Formulation of a general model. Contrib Mineral Petrol 116: 277–286

Sack RO, Ghiorso MS (1994b) Thermodynamics of multicomponent pyroxenes. II. Phase relations in the quadrilateral. Contrib Mineral Petrol 116: 287–300

Sack RO, Ghiorso MS (1994c) Thermodynamics of multicomponent pyroxenes. III. Calibration of $Fe^{2+}(Mg)_{-1}$, $TiAl_2(MgSi_2)_{-1}$, $TiFe_2^{3+}((MgSi_2)_{-1}$, $AlFe^{3+}(MgSi)_{-1}$, $Al_2(MgSi)_{-1}$, and $Ca(Mg)_{-1}$ exchange reactions between pyroxenes and silicate melts. Contrib Mineral Petrol 118: 271–296

Sack RO, Carmichael ISE, Walker D (1987a) Experimental petrology of alkalic lavas: constraints on cotectics of multiple saturation in natural basic. Contrib Mineral Petrol 96: 1–23

Sack RO, Ebel DS, O'Leary MJ (1987b) Tennahedrite thermochemistry and metal zoning. In: Helgeson HC (ed) Chemical transport in metasomatic processes. Reidel, Dordrecht, pp 701–731

Sahama THG (1957) Complex nepheline-kalsilite phenocrysts in Kabfumu lava, Nyiragongo area, North Kivu in Belgian Congo. J Geol 65: 515–526

Sahama THG (1962) Perthite-like exsolution in the nepheline-kalsilite system. Nor Geol Tidsskr 42(2): 168–179

Sahama THG, Smith JV (1957) Tri-kalsilite, a new mineral. Am Mineral 42: 286

Smith JV, Tuttle OF (1957) The nepheline-kalsilite system:I. X-ray data for the crystalline phases. Am J Sci 255: 282–305

Stebbins JF, Murdock JB, Carmichael ISE, Pines A (1986) Defects and short-range order in nepheline group minerals; a silicon 29 nuclear magnetic resonance study. Phys Chem Mineral 13: 371–381

Taylor WH (1930) The structure of analcite ($NaAlSi_2O_6 \cdot H_2O$). Z Kristallogr 74: 1–19

Thompson JB Jr, Hovis GL (1979) Structural-thermodynamic relations in the alkali feldspars. Trans Am Crystallogr Assoc 15: 1–15

Thompson JB Jr, Waldbaum DR (1969) Mixing properties of sanidine crystalline solutions: III. Calculations based on two-phase data. Am Mineral 54: 811–838

Tuttle OF, Smith JV (1958) The nepheline-kalsilite system: II. Phase relations. Am J Sci 256: 571–589

Waterwiese T, Chatterjee ND, Dierdorf I, Göttlicher J, Kroll H (1995) Experimental and thermodynamic study of heterogeneous and heterogeneous equilibria in the system $NaAl SiO_4$–SiO_2. Contrib Mineral Petrol 121: 61–73

Wyart MJ (1938) Étude sur la leucite. Bull Soc Fr Mineral 61: 228–38

Wyart MJ (1940) Étude cristallographique d'une leucite artificielle. Structure atomique et symétrie du minéral. Bull Soc Fr Mineral 63: 5–17

Zyrianov VN, Perchuk LL, Podlesskii KK (1978) Nepheline-alkali feldspar equilibria. I. Experimental data and thermodynamic calculations. J Petrol 19: 1–44